

# UC Irvine

## UC Irvine Previously Published Works

### Title

Zn<sup>2+</sup>-induced disruption of neuronal mitochondrial function: Synergism with Ca<sup>2+</sup>, critical dependence upon cytosolic Zn<sup>2+</sup> buffering, and contributions to neuronal injury

### Permalink

<https://escholarship.org/uc/item/9n03f0d4>

### Authors

Ji, Sung G  
Weiss, John H

### Publication Date

2018-04-01

### DOI

10.1016/j.expneurol.2018.01.012

Peer reviewed



Published in final edited form as:

*Exp Neurol.* 2018 April ; 302: 181–195. doi:10.1016/j.expneurol.2018.01.012.

## Zn<sup>2+</sup>-induced disruption of neuronal mitochondrial function: synergism with Ca<sup>2+</sup>, critical dependence upon cytosolic Zn<sup>2+</sup> buffering, and contributions to neuronal injury

Sung G. Ji<sup>1</sup> and John H. Weiss, MD, PhD<sup>1,2</sup>

<sup>1</sup>Department of Anatomy & Neurobiology, University of California, Irvine

<sup>2</sup>Department of Neurology, University of California, Irvine

### Abstract

Excitotoxic Zn<sup>2+</sup> and Ca<sup>2+</sup> accumulation contributes to neuronal injury after ischemia or prolonged seizures. Synaptically released Zn<sup>2+</sup> can enter postsynaptic neurons via routes including voltage sensitive Ca<sup>2+</sup> channels (VSCC), and, more rapidly, through Ca<sup>2+</sup> permeable AMPA channels. There are also intracellular Zn<sup>2+</sup> binding proteins which can either buffer neuronal Zn<sup>2+</sup> influx or release bound Zn<sup>2+</sup> into the cytosol during pathologic conditions. Studies in culture highlight mitochondria as possible targets of Zn<sup>2+</sup>; cytosolic Zn<sup>2+</sup> can enter mitochondria and induce effects including loss of mitochondrial membrane potential ( $\Psi_m$ ), mitochondrial swelling, and reactive oxygen species (ROS) generation. While brief (5 min) neuronal depolarization (to activate VSCC) in the presence of 300  $\mu$ M Zn<sup>2+</sup> causes substantial delayed neurodegeneration, it only mildly impacts acute mitochondrial function, raising questions as to contributions of Zn<sup>2+</sup>-induced mitochondrial dysfunction to neuronal injury.

Using brief high (90 mM) K<sup>+</sup>/Zn<sup>2+</sup> exposures to mimic neuronal depolarization and extracellular Zn<sup>2+</sup> accumulation as may accompany ischemia *in vivo*, we examined effects of disrupted cytosolic Zn<sup>2+</sup> buffering and/or the presence of Ca<sup>2+</sup>, and made several observations: **1.** Mild disruption of cytosolic Zn<sup>2+</sup> buffering—while having little effects alone—markedly enhanced mitochondrial Zn<sup>2+</sup> accumulation and dysfunction (including loss of  $\Psi_m$ , ROS generation, swelling and respiratory inhibition) caused by relatively low (10 – 50  $\mu$ M) Zn<sup>2+</sup> with high K<sup>+</sup>. **2.** The presence of Ca<sup>2+</sup> during the Zn<sup>2+</sup> exposure decreased cytosolic and mitochondrial Zn<sup>2+</sup> accumulation, but markedly exacerbated the consequent dysfunction. **3.** Paralleling effects on mitochondria, disruption of buffering and presence of Ca<sup>2+</sup> enhanced Zn<sup>2+</sup>-induced neurodegeneration. **4.** Zn<sup>2+</sup> chelation after the high K<sup>+</sup>/Zn<sup>2+</sup> exposure attenuated both ROS production and neurodegeneration, supporting the potential utility of delayed interventions. Taken together, these data lend credence to the idea that in pathologic states that impair cytosolic Zn<sup>2+</sup> buffering, slow uptake of Zn<sup>2+</sup> along with Ca<sup>2+</sup> into neurons via VSCC can disrupt the mitochondria and induce neurodegeneration.

Address correspondence to: John H. Weiss, MD, Ph.D., 2101 Gillespie Building, Department of Neurology, University of California, Irvine, Irvine, CA 92697-4292, Tel: (949) 824-6774, Fax: (949) 824-1668, jweiss@uci.edu.

**Publisher's Disclaimer:** This is a PDF file of an unedited manuscript that has been accepted for publication. As a service to our customers we are providing this early version of the manuscript. The manuscript will undergo copyediting, typesetting, and review of the resulting proof before it is published in its final citable form. Please note that during the production process errors may be discovered which could affect the content, and all legal disclaimers that apply to the journal pertain.

## Keywords

zinc; calcium; excitotoxicity; mitochondria; ischemia; neuronal cultures; VSCC; Ca<sup>2+</sup> channel; metallothionein; reactive oxygen species

---

## Introduction

Ischemic stroke is a leading cause of morbidity and mortality to the aging population, but no neuroprotective therapy exists, partly reflecting limited understanding of relevant injury mechanisms. Excitotoxicity, caused by excessive glutamate release, is considered to be a major contributor to neurodegeneration. Prior studies of excitotoxic injury have largely focused on rapid Ca<sup>2+</sup> entry through N-methyl-D-aspartate (**NMDA**) receptors, and have suggested mitochondria to be critical targets of the cellular Ca<sup>2+</sup> loads (Choi et al., 1988; Nicholls and Budd, 2000; Rothman and Olney, 1986), but NMDA receptor targeted therapies have shown limited clinical efficacy (Hoyte et al., 2004; Ikonomidou and Turski, 2002).

Additional studies have implicated another highly prevalent divalent cation, Zn<sup>2+</sup>, which accumulates in neurons after ischemia and prolonged seizures, and contributes to neurodegeneration (Frederickson et al., 1989; Koh et al., 1996; Tonder et al., 1990). Zn<sup>2+</sup> is stored in presynaptic vesicles, can be released upon activation, and enters postsynaptic neurons (“**Zn<sup>2+</sup> translocation**”) through routes including voltage sensitive Ca<sup>2+</sup> channels (**VSCC**) (Weiss et al., 1993), and with greater rapidity, through the subset of  $\alpha$ -amino-3-hydroxy-5-methyl-4-isoxazolepropionic acid channels that are both Ca<sup>2+</sup> and Zn<sup>2+</sup> permeable (**Ca-AMPA**) (Jia et al., 2002; Sensi et al., 1999a; Yin and Weiss, 1995). Zn<sup>2+</sup> has potent effects on isolated mitochondria (Brown et al., 2000; Dineley et al., 2005; Gazaryan et al., 2007; Jiang et al., 2001; Link and von Jagow, 1995; Sensi et al., 2003; Skulachev et al., 1967), and neuronal Zn<sup>2+</sup> loading triggered by rapid entry through Ca-AMPA channels induces acute mitochondrial dysfunction, including reactive oxygen species (**ROS**) generation (Sensi et al., 1999a; Sensi et al., 2000), with greater potency than Ca<sup>2+</sup>, suggesting that mitochondria might be critical targets of Zn<sup>2+</sup> effects. However, while slower Zn<sup>2+</sup> entry through VSCC caused considerable delayed neurodegeneration, these exposures had relatively little impact on acute mitochondrial function (Sensi et al., 1999a; Weiss et al., 1993), raising doubt that Zn<sup>2+</sup> translocation contributes importantly to mitochondrial dysfunction in pathological conditions (Pivovarova et al., 2014).

It is now apparent that in addition to direct entry of extracellular Zn<sup>2+</sup>, another critical determinant of cytosolic (and mitochondrial) Zn<sup>2+</sup> accumulation is the presence of Zn<sup>2+</sup> buffering proteins—like metallothioneins (**MTs**)—which normally buffer Zn<sup>2+</sup> loads, but can also provide a source from which bound Zn<sup>2+</sup> can be released by oxidative stress/acidosis, as can occur during pathological conditions (Malaiyandi et al., 2004; Maret, 2011; Maret and Vallee, 1998). Indeed, strong disruption of these intracellular Zn<sup>2+</sup> pools causes acute cytosolic and mitochondrial Zn<sup>2+</sup> accumulation even without Zn<sup>2+</sup> translocation (Sensi et al., 2003), and can trigger slow Zn<sup>2+</sup> dependent neuronal injury (Aizenman et al., 2000).

However, little is known about the respective contributions of each of these sources to mitochondrial dysfunction; indeed, only few studies to date have begun to explore the idea

that the integrity of cytosolic buffering may critically modulate the effects of exogenous  $Zn^{2+}$  entry on mitochondrial function in cultured neurons (Clausen et al., 2013; Sensi et al., 2003). Furthermore, as most early studies were carried out in  $Ca^{2+}$  free media to ensure observation of  $Zn^{2+}$  specific effects, there is debate about the respective contributions of  $Ca^{2+}$  and  $Zn^{2+}$  to mitochondrial dysfunction observed *in vivo*, with some proposing synergy between these ions (Gazaryan et al., 2007; Jiang et al., 2001; Sensi et al., 2000) while others see little evidence for  $Zn^{2+}$  contributions (Devinney et al., 2009; Pivovarova et al., 2014).

The present study seeks to model early  $Zn^{2+}$  dependent events in ischemic neuronal injury to quantitatively examine how disrupted cytosolic  $Zn^{2+}$  buffering and the presence of  $Ca^{2+}$  modulate the consequences of moderate exogenous  $Zn^{2+}$  loads on mitochondrial function and cell death. To this aim, we use brief high  $K^+/Zn^{2+}$  exposures (to mimic neuronal depolarization and extracellular  $Zn^{2+}$  accumulation as may accompany ischemia *in vivo*), and find that both disrupted buffering and the presence of  $Ca^{2+}$  strongly increase the impact of low  $Zn^{2+}$  exposures on mitochondrial function and cell death, with greater synergistic effects when combined. These findings support the hypothesis that slow  $Zn^{2+}$  entry into depolarized neurons could well contribute to mitochondrial dysfunction and neurodegeneration *in vivo*. Furthermore,  $Zn^{2+}$  chelation after the  $Zn^{2+}$  load diminishes both mitochondrial ROS generation and cell death, supporting the idea that delayed interventions targeting mitochondrial  $Zn^{2+}$  could provide therapeutic benefits.

## Material and methods

### Ethics statement

This study was carried out in accordance with the recommendations from the Guide for the Care and Use of Laboratory Animals of the National Institutes of Health and approved by the Institutional Animal Care and Use Committee of the University of California, Irvine.

### Cortical cultures

Primary mixed cortical cultures were prepared as described previously (Yin et al., 1994). Briefly, cell suspensions from neocortical regions of CD-1 mouse embryos (gender not determined) from 15–16 gestational day timed-pregnant mice (ordered from Charles River CrI:CD1[ICR]) were extracted and plated on astrocytic monolayers in glass-bottomed dishes, on culture treated 24 well microplates, or on Seahorse XF24 cell culture microplates. Cells were maintained in media consisting of Minimum Essential Medium (**MEM**) supplemented with 10% heat-inactivated horse serum, 10% fetal bovine serum, 2 mM glutamine, and 25 mM glucose, and kept in 37°C/5%  $CO_2$  incubator. 2–3 days after dissection, the cultures were switched to an identical maintenance medium lacking fetal bovine serum and non-neuronal cell division halted by adding 10  $\mu$ M cytosine arabinoside for 24 hrs. To prepare glial cultures (used to establish astrocytic monolayers described above), the same protocol was used, except the following: 1) tissues were obtained from 1–3 days old postnatal mice (gender not determined), 2) plating media was supplemented with epidermal growth factor (10 ng/ml), and 3) suspensions were directly plated on poly-D-lysine and laminin-coated coverslips and/or tissue culture treated plates.

## Reagents and indicators

Hydroethidine (**HEt**) was purchased from Assay Biotech (Sunnyvale, CA). Newport Green, FluoZin-3 AM, MitoTracker Green, Pluronic F-127, MEM, fetal bovine serum, glutamine, and horse serum were purchased from Life Technologies (Grand Island, NY). N-methyl-D-aspartate (**NMDA**), 2,2'-dithiodipyridine (**DTDP**), Rhodamine 123 (**Rhod123**), and N,N,N,N-tetrakis(2-pyridylmethyl)ethane-1,2-diamine (**TPEN**) were purchased from Sigma-Aldrich (St. Louis, MO). Carbonyl cyanide-p-trifluoromethoxyphenylhydrazone (**FCCP**) was purchased from Tocris Bioscience (Ellisville, MO), apocynin obtained from Acros Organics (Morris Plains, NJ), and XF Base Medium (minimal Dulbecco's Modified Eagle's Medium) from Agilent Technologies (Santa Clara, CA). All other chemicals and reagents were purchased from common commercial sources.

## Zn<sup>2+</sup>/Ca<sup>2+</sup> loading

Prior to all experiments, cultured neurons were removed from the incubator and placed in HEPES-buffered media (consisting of [in mM] 120 NaCl, 5.4 KCl, 0.8 MgCl<sub>2</sub>, 20 Hepes, 15 glucose, 10 NaOH, in pH 7.4) with either 1.8 mM CaCl<sub>2</sub> (**1.8 Ca<sup>2+</sup> HSS**) or 0 mM CaCl<sub>2</sub> (**0 Ca<sup>2+</sup> HSS**) at room temperature. Cultures were maintained in HSS ( $\pm$  Ca<sup>2+</sup>) for 10 min, followed where indicated by addition of "pre-treatment" (with DTDP and/or TPEN) for 10 min prior to induction of Zn<sup>2+</sup> and/or Ca<sup>2+</sup> loading. To do so, neurons were exposed to indicated levels of Zn<sup>2+</sup> (0 – 300  $\mu$ M) and/or 1.8 mM Ca<sup>2+</sup> in 90 mM K<sup>+</sup> HSS ("**high K<sup>+</sup>**"; HSS modified with 90 mM K<sup>+</sup> and Na<sup>+</sup> adjusted to 35 mM to maintain osmolarity) for 5 min to depolarize neurons, inducing ion entry through VSCC. When Ca<sup>2+</sup> was present during exposure (with or without Zn<sup>2+</sup>), the NMDA antagonist MK-801 (10  $\mu$ M) was added to inhibit Ca<sup>2+</sup> entry through NMDA receptors. After the 5 min exposure in high K<sup>+</sup>, neurons were washed 3 times into HSS ( $\pm$  Ca<sup>2+</sup>, DTDP and TPEN as present before the exposure) for durations indicated. In addition, as we have found highly Ca<sup>2+</sup> or Zn<sup>2+</sup> permeable Ca-AMPA channels to be expressed in a small subset (~ 13%) of cultured cortical neurons (Yin et al., 1994), we carried out additional controls using the AMPA channel antagonist 2,3-dihydroxy-6-nitro-7-sulfamoyl-benzo(F)quinoxaline (NBQX; 10  $\mu$ M) during the exposures (Sensi et al., 1999a), and found no differences.

## Quantitative imaging studies

10–16 days in vitro (**DIV**) cultures were mounted on the stage of a Nikon Diaphot inverted microscope equipped with a 75 W xenon lamp, a computer-controlled filter wheel, a 40x (1.3 numerical aperture) epifluorescence oil-immersion objective along with a green FITC fluorescence cube (Ex: 480 nm, dichroic: 505 nm, Em: 535 nm) and a red TRITC fluorescence cube (Ex: 540 nm, dichroic: 565 nm, Em: 605 nm). Emitted signals were acquired once every min with a Sensys Photometrics intensified charge-coupled device camera and digitized through the MetaFluor Version 7.0 software (Molecular Devices LLC, Sunnyvale, CA). Camera gain and exposure were adjusted to give baseline maximal fluorescence levels of 200–300 arbitrary units of a maximal 12-bit signal output of 4,096 for all fluorophores. While the precise experiment schematic is described below, generally, baseline was measured for 10 min, followed by 10 min pre-treatment with DTDP and/or TPEN (if indicated), then by 5 min Zn<sup>2+</sup> and/or Ca<sup>2+</sup> loading (with high K<sup>+</sup>), and finally by

wash into HSS, with addition of FCCP if indicated. For imaging, fields with 15 healthy looking cells (defined as non-clustered neurons with robust processes), were selected. Background fluorescence (defined as the lowest fluorescence value in a neuron free region of the field) was subtracted from images, and fluorescence measurements for each cell ( $F_x$ ) were normalized to the average fluorescence intensity of the 10 min baseline recording ( $F_0$ ) to track normalized fluorescence ( $F_x/F_0$ ) over time.  $F_x/F_0$  of each cell from the field was averaged to produce one value, constituting one repetition of an experiment.

To assess cytosolic  $Zn^{2+}$  levels, cultures were first loaded in the dark with 5  $\mu M$  of either the low affinity  $Zn^{2+}$  indicator, Newport Green diacetate ( $K_d \sim 1 \mu M$ , Ex: 490 nm, Em: 530 nm), or the high affinity  $Zn^{2+}$  indicator FluoZin-3 AM ( $K_d \sim 15$  nM, Ex: 494 nm, Em: 516 nm) in 0  $Ca^{2+}$  HSS containing 0.2 % Pluronic F-127 and 1.5 % dimethyl sulfoxide for 30 min at room temperature, then washed into 1.8  $Ca^{2+}$  HSS and kept in the dark for additional 30 min at room temperature to de-esterify indicators prior to imaging (using a green FITC fluorescence cube). Mitochondrial membrane potential ( $\Psi_m$ ) was assessed by examining fluorescence changes in Rhod123 (Ex: 507 nm, Em: 529 nm), a positively charged dye that accumulates in active mitochondria, where its fluorescence intensity is quenched. Upon loss of  $\Psi_m$ , Rhod123 is released into the cytosol, resulting in increased fluorescence (Duchen et al., 2003). Neurons were incubated in the dark with 2  $\mu M$  of Rhod123 in 1.8  $Ca^{2+}$  HSS for 30 min in room temperature prior to imaging (using a green FITC fluorescence cube). At the end of each experiment, the mitochondrial protonophore FCCP was added (1  $\mu M$ , 5 min) to induce maximal loss of  $\Psi_m$  (and record the corresponding maximal Rhod123  $F$ ). ROS generation was assessed using the superoxide sensitive dye HET (Ex: 510–560 nm; Em: > 590 nm; using a red TRITC fluorescence cube). Cultures were loaded in the dark at room temperature with 5  $\mu M$  HET in either 0 or 1.8  $Ca^{2+}$  HSS for 30 min prior to imaging; ROS production is assessed as the rate of fluorescence increase (HET  $F$ ) as the HET is oxidized into highly fluorescent ethidium.

### Confocal imaging of mitochondrial morphology

Confocal microscopy of mitochondrial morphology was performed using an inverted stage Nikon Eclipse Ti chassis microscope with a Yokogawa CSUX spinning disk head. Images were collected with a 1000x (1.49 numerical aperture) oil-immersion objective using a Hamamatsu electromultiplying CCD camera, scanned sequentially with excitation (488 nm) via a Coherent sapphire laser source synchronized with the camera, and emission monitored with a 525 (50) nm filter, and acquired using MicroManager Image Acquisition software (version 1.4.16). Briefly, cells were loaded with 200 nM MitoTracker Green (Ex: 490 nm, Em: 516 nm) in 1.8  $Ca^{2+}$  HSS for 30 min at room temperature in the dark, and then switched to either 0 or 1.8  $Ca^{2+}$  HSS for the imaging experiment. Imaging rig was maintained at 37°C via heat fan, and camera gain, laser power, and exposure times were adjusted to give baseline fluorescence intensity of MitoTracker Green approximately 1.5x that of the background fluorescence value. Healthy looking neuron(s) were selected for imaging and exposed to treatments as described. Images were taken at baseline, 10 min after DTDP (if used), 5 min after  $Zn^{2+}$  and/or  $Ca^{2+}$  exposure and 10 min after wash (as detailed in Fig. 6). Acquired images were blinded to both treatment groups and time points, then imported into ImageJ software, which was used to make adjustment to whole image to provide optimal

discrimination of mitochondrial morphology. Lengths and width of distinct mitochondria were measured manually, the values of which were then used to calculate the length/width (L/W) ratio of the mitochondria. To assess relative changes in morphology over time, the L/W ratio was normalized to baseline values. The L/W ratios of the mitochondria found in the selected field were averaged to produce one average L/W ratio, representing one repetition of an experiment.

### Mitochondrial respiration assay

Mitochondrial respiration was assessed by measuring changes in O<sub>2</sub> consumption rate (OCR) using the Seahorse XF24 Extracellular Flux Analyzer, as described previously with adjustments (Yao et al., 2009). Briefly, neurons plated on top of astrocytic monolayers on Seahorse XF24 Cell Culture Microplates were exposed to DTDP, Zn<sup>2+</sup> and/or Ca<sup>2+</sup> in either 0 or 1.8 Ca<sup>2+</sup> HSS (as detailed in Fig. 7), washed into XF Base Medium (supplemented with 2 mM glutamine, 15 mM glucose, and 1 mM sodium pyruvate), and maintained at 37°C for 1 hr. After the 1 hr incubation, the cultures were placed in the Seahorse XF24 instrument, which measures the OCR of cells during baseline and after the sequential exposure to 1 μM oligomycin, 2 μM FCCP, and antimycin A/rotenone (both at 1 μM). The concentrations of oligomycin, FCCP, and antimycin A/rotenone were based on those from the literature (Yao et al., 2009) as well as empirical titration, with FCCP specifically adjusted to induce at least 1.5x the baseline OCR. Prior to each experiment, Seahorse XF24 instrument was calibrated following the manufacturer's protocols, and all culture wells were visually inspected (to ensure equal distribution of cells) and randomly assigned to treatment groups. Seahorse XF24 program was used to run the assay and Seahorse Wave Software used to analyze data. As neurons were plated on pre-established astrocyte monolayers (using the same culturing methods as described above), we carried out validation studies comparing responses of neuron-astrocyte co-culture to those of astrocyte-only cultures, confirming that astrocytes made minimal (~5%) contributions to observed basal OCR and OCR changes (data not shown).

### Assessment of cell death

Cell death was assessed in neurons plated on culture treated 24 well microplates. Briefly, 14–16 DIV neurons were switched into 0 or 1.8 Ca<sup>2+</sup> HSS, and exposed to a combination of DTDP, TPEN, Ca<sup>2+</sup> and/or Zn<sup>2+</sup> (concentration and durations detailed below). Cultures were then washed into MEM supplemented with 25 mM glucose and kept at 37°C/5% CO<sub>2</sub> for 24 hrs (unless otherwise specified), prior to assessment of neuronal injury via direct examination (under phase-contrast microscopy) and by lactate dehydrogenase (LDH) efflux assay as described (Koh and Choi, 1987). The small amount of background LDH present in the media of cultures carried through a sham-wash protocol was subtracted from values obtained in treated cultures. In each experiment, LDH values were scaled to the mean value obtained by a standard exposure to 300 μM NMDA for 24 hr (an exposure that reliably destroys most of the neuronal population without glial damage).



## Statistical analysis and repetition

To assess significance, either two-tailed t-test or one-way ANOVA with Tukey post-hoc analysis (indicated in each figure legend) was used, depending on the number of groups of comparison. All values are displayed as mean  $\pm$  standard error of the mean (SEM). All experiments were repeated at least 3 times. Note that because of some differences in precise behavior of batches of cells reflecting biologic variables—including age and health—all comparisons reflect matched sets of cells, using the same sets of culture dissections with interleaved experiments.

## Results

### Slow Zn<sup>2+</sup> translocation through VSCC induces only mild mitochondrial dysfunction

As discussed above, neuronal Zn<sup>2+</sup> accumulation contributes to delayed neurodegeneration in pathological conditions like ischemia. One likely important source of this Zn<sup>2+</sup> is co-release (with glutamate) from presynaptic terminals, and its entry into postsynaptic neurons (“translocation”) via various routes (including VSCC and Ca-AMPA channels). Inside neurons, Zn<sup>2+</sup> can enter mitochondria and disrupt their function (Clausen et al., 2013; Jiang et al., 2001; Sensi et al., 2003; Sensi et al., 2002; Sensi et al., 2000). While mitochondrial Ca<sup>2+</sup> accumulation has long been considered the major contributor to their dysfunction in ischemia (Halestrap, 2006; Nicholls and Budd, 2000), clues have emerged that Zn<sup>2+</sup> may also be an important contributor (Bonanni et al., 2006; Calderone et al., 2004; Medvedeva et al., 2017; Medvedeva et al., 2009; Medvedeva and Weiss, 2014), particularly after rapid influx through highly Zn<sup>2+</sup> permeable Ca-AMPA channels (Jia et al., 2002; Sensi et al., 1999a; Yin and Weiss, 1995). However, although brief exposure of cultured neurons to Zn<sup>2+</sup> under depolarizing conditions (triggering entry largely through VSCC) led to considerable delayed degeneration (Weiss et al., 1993), this induced only mild acute effects on mitochondria (Pivovarova et al., 2014; Sensi et al., 1999a), raising uncertainty as to contributions of slower Zn<sup>2+</sup> translocation to mitochondrial dysfunction in disease conditions.

Present studies seek to further clarify whether and under what circumstances low to moderate extracellular Zn<sup>2+</sup> accumulation and its slower entry into neurons can impact the mitochondria and promote neuronal injury. We chose to model Zn<sup>2+</sup> translocation by inducing entry through the VSCC, as may occur in ischemia with extracellular Zn<sup>2+</sup> accumulation around depolarized neurons, because VSCC are ubiquitously expressed (unlike Ca-AMPA channels, which are only present on some neurons) and permit slower entry, resulting in more uniform and moderate Zn<sup>2+</sup> loads. Our first aim was to extend prior studies by quantitatively examining the relationship between extracellular Zn<sup>2+</sup> exposure, cytosolic and mitochondrial Zn<sup>2+</sup> accumulation, and the consequent acute mitochondrial dysfunction.

Neurons were loaded with the low affinity cytosolic Zn<sup>2+</sup> indicator Newport Green ( $K_d \sim 1 \mu\text{M}$ ) (Sensi et al., 1999a) in 0 Ca<sup>2+</sup> HSS (to ensure observation of Zn<sup>2+</sup>-specific effects). After measuring baseline fluorescence for 10 min, cultures were exposed to 25, 75, or 300  $\mu\text{M}$  Zn<sup>2+</sup> with high (90 mM) K<sup>+</sup> for 5 min, washed into 0 Ca<sup>2+</sup> HSS for 5 min, then treated



to the mitochondrial protonophore, carbonyl cyanide 4-(trifluoromethoxy)phenylhydrazone (**FCCP**, 1  $\mu\text{M}$ ) for 10 min. FCCP dissipates the proton gradient across the inner mitochondrial membrane, resulting in rapid loss of mitochondrial membrane potential ( $\Psi_m$ ) and release of mitochondrially sequestered  $\text{Zn}^{2+}$  (Clausen et al., 2013; Medvedeva et al., 2017; Sensi et al., 2003; Sensi et al., 2002). Thus, the rise in cytosolic  $\text{Zn}^{2+}$  after FCCP (assessed as Newport Green fluorescence change; **Newport Green F**) reflects the amount of  $\text{Zn}^{2+}$  that had been taken up into mitochondria. Our findings indicate a direct relationship between the magnitude of the exogenous  $\text{Zn}^{2+}$  load with both the degree of cytosolic  $\text{Zn}^{2+}$  rise and the consequent  $\text{Zn}^{2+}$  uptake into mitochondria (Fig. 1A), with high  $\text{K}^+$ /300  $\mu\text{M}$   $\text{Zn}^{2+}$  exposure resulting in far greater cytosolic and mitochondrial  $\text{Zn}^{2+}$  accumulation than the 25 or 75  $\mu\text{M}$  exposures.

We next sought to examine the acute consequences of these mitochondrial  $\text{Zn}^{2+}$  loads on  $\Psi_m$  and reactive oxygen species (**ROS**) generation. To assess changes in  $\Psi_m$ , we used the cationic indicator Rhodamine 123 (**Rhod123**), which accumulates in mitochondria in proportion to their  $\Psi_m$  (where its fluorescence is quenched); upon loss of  $\Psi_m$ , Rhod123 is released into the cytosol and the fluorescence increases (**Rhod123 F**) (Duchen et al., 2003). ROS generation was assessed using the superoxide preferring oxidant sensitive indicator, hydroethidine (**HEt**), which is oxidized by superoxide radicals into the highly fluorescent compound, ethidium. The fluorescence of ethidium is amplified upon its binding to DNA, providing high sensitivity and resulting in predominant visualization of the signal in the nucleus (Bindokas et al., 1996). Because the oxidized ethidium accumulates, the rate of fluorescence increase indicates ROS production rate, and the increase in HEt fluorescence (**HEt F**) over baseline reflects total ROS production. Rhod123 and HEt loaded cultures were exposed to  $\text{Zn}^{2+}$  in high  $\text{K}^+$  and washed into 0  $\text{Ca}^{2+}$  HSS, similarly as above. After the 300  $\mu\text{M}$   $\text{Zn}^{2+}$  exposures, we detected modest loss of  $\Psi_m$  (as indicated by Rhod123 F prior to FCCP-induced maximal depolarization) and ROS production (as indicated by HEt F); the 25 and 75  $\mu\text{M}$   $\text{Zn}^{2+}$  exposures had little effects (Fig. 1B). Of note, although  $\text{Zn}^{2+}$  exposure has been found to cause delayed activation of the superoxide generating enzyme NADPH oxidase (**NOX**) (Noh and Koh, 2000), our prior studies indicated that rapid  $\text{Zn}^{2+}$  triggered ROS production is almost entirely of mitochondrial origin (Clausen et al., 2013; Sensi et al., 1999a). Thus, above data suggest that while neuronal  $\text{Zn}^{2+}$  entry through VSCC (modeling slow  $\text{Zn}^{2+}$  translocation) induces dose dependent mitochondrial  $\text{Zn}^{2+}$  accumulation, acute mitochondrial dysfunction was only detected with the strongest (300  $\mu\text{M}$ )  $\text{Zn}^{2+}$  exposures.

### Critical role of cytosolic buffering in $\text{Zn}^{2+}$ -triggered mitochondrial dysfunction

We next sought to examine the degree to which endogenous  $\text{Zn}^{2+}$  buffering, likely in large part via MTs, impacts  $\text{Zn}^{2+}$  dependent modulation of mitochondrial function. Indeed, whereas  $\text{Zn}^{2+}$  mobilization from cytosolic buffers appears able to impact mitochondrial function and trigger slow  $\text{Zn}^{2+}$  dependent injury even in the absence of exogenous  $\text{Zn}^{2+}$  entry (Aizenman et al., 2000; Sensi et al., 2003), there has been little quantitative assessment of these effects. To disrupt endogenous  $\text{Zn}^{2+}$  buffering, we used the disulfide compound 2,2-dithiodipyridine (DTDP) which oxidizes the sulfhydryls linking  $\text{Zn}^{2+}$  to cysteines, thus

releasing bound  $Zn^{2+}$  from buffering proteins (like MTs) and preventing the released  $Zn^{2+}$  from being bound again (Aizenman et al., 2000; Maret and Vallee, 1998; Sensi et al., 2003).

To assess  $Zn^{2+}$  release from the buffers and its ability to enter mitochondria, we loaded cells (in 0  $Ca^{2+}$  HSS) with the higher affinity  $Zn^{2+}$  indicator, FluoZin-3 ( $K_d \sim 15$  nM) (Gee et al., 2002; Sensi et al., 2003), and monitored changes in fluorescence before and after application of 100  $\mu$ M DTDP and subsequent addition of FCCP. In agreement with our prior observations (Sensi et al., 2003), this fairly high DTDP exposure caused a prompt but relatively modest  $Zn^{2+}$  rise, followed by a further sharp rise in cytosolic  $Zn^{2+}$  upon FCCP exposure, indicating robust mitochondrial  $Zn^{2+}$  accumulation (likely due to strong disruption of cytosolic buffering). With lower (60  $\mu$ M) DTDP, we still observed an acute cytosolic  $Zn^{2+}$  rise and mitochondrial  $Zn^{2+}$  uptake, but these were markedly diminished, consistent with impaired—but not fully disrupted— $Zn^{2+}$  buffering (Fig. 2A).

To examine acute effects of these DTDP exposures on mitochondria, we used the  $\Psi_m$  indicator Rhod123 and the ROS indicator HET, as above. With continuous exposure to 100  $\mu$ M DTDP, we noted a gradual increase in Rhod123  $\Delta F$  that progressed to subtotal loss of  $\Psi_m$  within 40 min (as indicated by lack of response to FCCP), and a rise in HET  $\Delta F$  indicative of increased ROS production. In contrast, with 60  $\mu$ M DTDP, there was little Rhod123 or HET  $\Delta F$  (Fig. 2B). Finally, to validate the  $Zn^{2+}$  dependence of these DTDP effects, we repeated strong (100  $\mu$ M) DTDP exposures in the presence or absence of the membrane permeable  $Zn^{2+}$  chelator, N,N,N,N-tetrakis(2-pyridylmethyl)ethane-1,2-diamine (TPEN; 20  $\mu$ M, applied 10 min before and with DTDP). TPEN application provided near complete block of both the Rhod123 and HET  $\Delta F$ , indicating that the acute effects of the DTDP exposure on mitochondrial function are largely  $Zn^{2+}$  dependent, likely resulting from movement of  $Zn^{2+}$  from the endogenous buffers into the mitochondria (Fig. 2C). (As prior studies found DTDP to promote mild  $Ca^{2+}$  release from endoplasmic reticulum (McCord and Aizenman, 2013), we assessed effects of DTDP exposures on  $Ca^{2+}$ , and confirmed very small rises that did not differ between 60 and 100  $\mu$ M DTDP exposures; data not shown). Thus, these results confirm and extend prior studies (Sensi et al., 2003), and indicate dose dependent effects of protracted mobilization of endogenous  $Zn^{2+}$  stores on mitochondria, even in the absence of extracellular  $Zn^{2+}$  influx.

While above findings help clarify the degree to which the integrity of cytosolic  $Zn^{2+}$  buffering can impact mitochondria, in pathological conditions like ischemia, disruption of buffering (due to acidosis/oxidative stress) would most likely occur concurrently with extracellular  $Zn^{2+}$  accumulation (largely from vesicular release). Thus, we next sought to examine how relatively low extracellular  $Zn^{2+}$  accumulation (at levels that may occur in ischemia) can impact mitochondria when cytosolic  $Zn^{2+}$  buffering is impaired. To this aim, we combined two exposures that each caused little acute mitochondrial dysfunction when applied alone (modest  $Zn^{2+}$  entry triggered by 5 min high  $K^+$  exposure with 50  $\mu$ M  $Zn^{2+}$ , and partial disruption of buffering induced by 60  $\mu$ M DTDP), and compared the consequences with those of a far greater exogenous  $Zn^{2+}$  exposure alone (high  $K^+$ /300  $\mu$ M  $Zn^{2+}$  in the absence of DTDP; see Fig. 1B, 2B). Using Newport Green, Rhod123, and HET to assess mitochondrial  $Zn^{2+}$  loading, loss of  $\Psi_m$  and ROS generation respectively (as in Fig. 1), we found these exposures to induce similar cytosolic rises and levels of acute

mitochondrial  $Zn^{2+}$  accumulation (as indicated by the similar Newport Green  $F$  upon adding FCCP; Fig. 3A), but the combined exposure caused markedly greater loss of  $\psi_m$  and ROS generation than the higher  $Zn^{2+}$  exposure alone (Fig. 3B, C). Furthermore, the loss of  $\psi_m$  and ROS generation occurring after the high  $K^+/50 \mu M Zn^{2+}/DTDP$  exposure are not transient, but appeared to progress at a near constant rate (as indicated by the slope of the Rhod123 and HET  $F$  traces) for the duration of the recording period. Prior studies have estimated that peak cytosolic  $Zn^{2+}$  rises after brief exposure to high  $K^+/300 \mu M Zn^{2+}$  are in the 100s of nM (a substantial increase from subnanomolar resting levels) (Canzoniero et al., 1999; Colvin et al., 2010; Frederickson et al., 2005; Maret, 2015; Sensi et al., 1999a). Thus, despite similar degrees of acute cytosolic and mitochondrial  $Zn^{2+}$  accumulation triggered by these exposures, the greater and longer-lasting mitochondrial dysfunction triggered by the lower exposure with DTDP likely reflects a greater persistence of the  $Zn^{2+}$  within the mitochondria, due to impaired ability to buffer the  $Zn^{2+}$  rises and recover  $Zn^{2+}$  homeostasis.

Finally, we examined the  $Zn^{2+}$  exposure dependence of the combined high  $K^+/Zn^{2+}/60 \mu M$  DTDP exposures by comparing effects obtained using  $50 \mu M Zn^{2+}$  with those occurring with lower ( $10 \mu M$ )  $Zn^{2+}$  exposures. Not surprisingly, the effects were strongly dose dependent, with the higher exposure causing more mitochondrial  $Zn^{2+}$  accumulation (Fig. 4A) and greater acute effects on  $\psi_m$  and ROS generation (Fig. 4B, C). Interestingly, the difference was greater for the ROS generation, with both exposures only causing partial loss of  $\psi_m$ . In sum, above data indicate that even partial disruption of cytosolic  $Zn^{2+}$  buffering can significantly exacerbate the impact of neuronal  $Zn^{2+}$  entry on mitochondria, and thus is likely to be a critical determinant of the extent of  $Zn^{2+}$ -triggered mitochondrial disruption after ischemia.

### **Ca<sup>2+</sup> reduces Zn<sup>2+</sup> uptake but exacerbates consequent mitochondrial dysfunction**

Above experiments (like many prior studies of  $Zn^{2+}$  effects) were carried out in  $Ca^{2+}$  free media, to ensure  $Zn^{2+}$ -specificity of effects. However, as  $Ca^{2+}$  is always present *in vivo*, we felt it crucial to next examine effects of  $Zn^{2+}$  in the presence of physiologic (1.8 mM) levels of  $Ca^{2+}$ . First, to assess effects of  $Ca^{2+}$  on cytosolic and mitochondrial  $Zn^{2+}$  accumulation, Newport Green loaded cultures were subjected to a range of  $Zn^{2+}$  loads (high  $K^+/300 \mu M Zn^{2+}$  alone, or high  $K^+$  with 10 or  $50 \mu M Zn^{2+}/60 \mu M$  DTDP) for 5 min in 0 or 1.8  $Ca^{2+}$  HSS. The NMDA antagonist, MK-801 (10  $\mu M$ ) was added during these exposures to prevent rapid  $Ca^{2+}$  influx through highly  $Ca^{2+}$  permeable NMDA channels. In each of these conditions, the presence of  $Ca^{2+}$  decreased both the cytosolic  $Zn^{2+}$  rises (likely reflecting competition for entry through VSCC) (Kerchner et al., 2000; Weiss et al., 1993) and the mitochondrial  $Zn^{2+}$  uptake (assessed as the  $F$  upon application of FCCP; Fig. 5A).

Despite above findings of reduced mitochondrial  $Zn^{2+}$  loading in the presence of  $Ca^{2+}$ , some prior studies have suggested that these ions may have synergistic effects on mitochondrial function (Gazaryan et al., 2007; Jiang et al., 2001; Sensi et al., 2000). Thus, we next used Rhod123 and HET loaded cultures to examine how the presence of  $Ca^{2+}$  influences  $Zn^{2+}$  effects on  $\psi_m$  and ROS generation. To assess possible synergism, we first examined the low end of the  $Zn^{2+}$  exposure range (high  $K^+$  with  $10 \mu M Zn^{2+}/60 \mu M$  DTDP) that caused little loss of  $\psi_m$  and ROS generation in 0  $Ca^{2+}$  HSS (Fig. 4B). In a new set of experiments,

cultures were exposed to high  $K^+$ /60  $\mu$ M DTDP (with 10  $\mu$ M MK-801) in the presence of either 10  $\mu$ M  $Zn^{2+}$ , 1.8 mM  $Ca^{2+}$  or with both  $Zn^{2+}$  and  $Ca^{2+}$ . In addition, as NOX activation has been reported to contribute, along with mitochondria, to acute  $Ca^{2+}$  triggered ROS generation (unlike acute  $Zn^{2+}$  triggered ROS, which, as discussed above, appears mostly to be of mitochondrial origin) (Brennan et al., 2009; Clausen et al., 2013), the NOX inhibitor apocynin (500  $\mu$ M) was added in HET loaded cultures to prevent ROS generation due to  $Ca^{2+}$  dependent activation of this enzyme. While the high  $K^+$  exposures with either the 10  $\mu$ M  $Zn^{2+}$  or 1.8 mM  $Ca^{2+}$  alone had little acute impact on the mitochondria, the combined exposure resulted in substantially greater loss of  $\psi_m$  and ROS generation (Fig. 5B), further substantiating the synergistic effects of  $Ca^{2+}$  and  $Zn^{2+}$  on mitochondria.

Finally, we examined the dose dependence of loss of  $\psi_m$  and ROS generation at the high end of the exposure range, in light of our prior observations (Fig. 4B, C) that high  $K^+$ /50  $\mu$ M  $Zn^{2+}$ /60  $\mu$ M DTDP exposures caused substantial ROS generation but rather modest loss of  $\psi_m$ . Rhod123 and HET loaded cultures were exposed to high  $K^+$  with  $Zn^{2+}$  (50 or 300  $\mu$ M) and 1.8 mM  $Ca^{2+}$  in 60  $\mu$ M DTDP (with MK-801, and apocynin added in HET loaded cultures as above). Whereas both of these exposures caused similar strong and persistent ROS generation, there was a clear dose dependency on the loss of  $\psi_m$ , with the 50  $\mu$ M  $Zn^{2+}$  exposure still causing only partial loss of  $\psi_m$ , while the “maximal” (and likely supraphysiological) 300  $\mu$ M  $Zn^{2+}$  exposure triggered near complete loss of  $\psi_m$  (Fig. 5C). This highlights the ability of mitochondria to maintain at least partial  $\psi_m$  despite quite strong  $Zn^{2+}$  loads that cause strong and persistent ROS generation.

Thus, despite the presence of  $Ca^{2+}$  in the extracellular fluid resulting in decreased cytosolic and mitochondrial  $Zn^{2+}$  accumulation, it markedly increases the consequent  $Zn^{2+}$  effects on the mitochondria, highlighting strong synergism of these 2 cations. Indeed, the degree of synergism is sufficient that even a quite brief and low extracellular  $Zn^{2+}$  exposure (5 min, 10  $\mu$ M  $Zn^{2+}$ ) applied under pathophysiologically relevant conditions (with  $Ca^{2+}$  present in depolarized neurons with partially impaired  $Zn^{2+}$  buffering) triggered substantial acute effects on the mitochondria.

### **Mitochondrial $Zn^{2+}$ accumulation induces rapid swelling and disruption of mitochondrial respiration**

Above findings lend credence to the hypothesis that neuronal  $Zn^{2+}$  entry contributes to mitochondrial dysfunction in pathological conditions like ischemia. However, whereas the measures employed thus far (loss of  $\psi_m$  and ROS production) are valuable indices of acute disruption, they are not indicative of long lasting mitochondrial dysfunction or loss of viability that may ultimately lead to neurodegeneration.

To address this, we first examined acute changes in mitochondrial morphology triggered by  $Zn^{2+}$  loads. While mitochondria are mostly rod shaped, in pathological conditions like ischemia, both  $Ca^{2+}$  and  $Zn^{2+}$  can trigger either transient or irreversible morphologic changes, including swelling (Brustovetsky et al., 2002; Halestrap, 2006; Jiang et al., 2001; Sugawara et al., 1999).

To assess mitochondrial morphology, cultures were loaded with the fluorescent mitochondrial marker, MitoTracker Green (200 nM), and neuronal mitochondria examined using confocal microscopy at 1000x (as described in Material and methods). This marker has the advantages that it covalently binds to mitochondrial proteins (and thus stays in neuronal mitochondria despite loss of  $\psi_m$ ) and maintains fluorescence in oxidative environments (Buckman et al., 2001; Jiang et al., 2001). Cultures were exposed as indicated to high  $K^+$ /MK-801 with  $Zn^{2+}$  and/or  $Ca^{2+}$  ( $\pm$  DTDP) and images acquired at baseline, after the 5 min  $Zn^{2+}/Ca^{2+}$  exposure, and, finally, 10 min after wash (into HSS  $\pm$  DTDP) (as indicated in Fig. 6A, B). We examined effects of 60  $\mu$ M as well as 100  $\mu$ M DTDP, to assess possible consequences of  $Zn^{2+}$  loads with both partial and near maximal disruption of cytosolic buffering, as might occur during episodes of strong *in vivo* ischemia. To assess morphological changes, images were blinded to experimental condition and time point, and imported into Image J software, where the lengths and widths of distinct mitochondria were measured manually (see Material and methods); data are expressed as mean length/width (L/W) ratios normalized to baseline values (which ranged from 4–8; mean  $5.9 \pm 0.3$ ).

There were distinct differences triggered by the different exposures (Fig. 6C): 1). Exposure to high  $K^+$ /1.8 mM  $Ca^{2+}$  alone caused a significant swelling of mitochondria evident at the end of the 5 min exposure, that had largely recovered after 10 min wash. 2). High  $K^+$  with 300  $\mu$ M  $Zn^{2+}$  alone, or with 50  $\mu$ M  $Zn^{2+}$ /60  $\mu$ M DTDP (both in 0  $Ca^{2+}$  HSS) did not cause swelling evident at the end of the exposure, but mild swelling was evident 10 min later in both treatments. 3). High  $K^+$ /50  $\mu$ M  $Zn^{2+}$ /100  $\mu$ M DTDP exposures in 0  $Ca^{2+}$  HSS caused marked swelling at the end of the exposure that substantially progressed over the subsequent 10 min; with  $Ca^{2+}$  present, the swelling at both time points was even greater, with extreme rounding up of mitochondria that may be indicative of irrecoverable damage. Of note, we found little morphological changes after 10 min pre-treatment with DTDP (60 or 100  $\mu$ M in 0 or 1.8  $Ca^{2+}$  HSS) prior to  $Zn^{2+}$  exposure (data not shown), further supporting the need for contributions from both extracellular  $Zn^{2+}$  entry and intracellular  $Zn^{2+}$  mobilization to potentially impact the mitochondria. In summary, these data suggest distinct effects of these ions, with  $Ca^{2+}$  being an effective trigger of acute transient—but largely recoverable—swelling, while  $Zn^{2+}$  induces swelling of slower onset, that, when “strengthened” (by DTDP and synergism with  $Ca^{2+}$ ) appears to be strongly progressive after termination of the exposure.

We next sought to examine delayed effects of the  $Zn^{2+}$  exposures on mitochondrial respiration. Indeed, as the main function of mitochondria is energy production, which is dependent upon the integrity of the electron transport chain, we felt it critical to assess such effects, which, in contrast to loss of  $\psi_m$  and ROS production, provide a direct measure of the disruption of mitochondrial respiratory capacity after an insult. For these studies, we made use of a device (the Seahorse XF24 analyzer) which measures the  $O_2$  consumption rate (OCR) in cultures at baseline and in response to sequential application of the following drugs: (1) the ATP synthase inhibitor, oligomycin (1  $\mu$ M), which prevents dissipation of the proton gradient across the inner membrane due to ATP synthesis, leading to membrane hyperpolarization and slowing of electron transport; the decrease in OCR upon its application provides an estimate of the portion of  $O_2$  consumption contributing to ATP

production; (2) FCCP (2  $\mu\text{M}$ ), which dissipates the proton gradient, uncoupling the electron transport chain, yielding maximal oxidative capacity and OCR, and; (3) combined application the complex I blocker, rotenone, and the complex III blocker, antimycin A (both 1  $\mu\text{M}$ ), to fully inhibit the electron transport chain, and blocking all mitochondrial respiration (Fig. 7A) (Brand and Nicholls, 2011).

We carried out two sets of experiments. The first aimed to examine synergism between effects of  $\text{Zn}^{2+}$  and  $\text{Ca}^{2+}$  (via exposure to high  $\text{K}^+$ /MK-801 with 300  $\mu\text{M}$   $\text{Zn}^{2+}$ , 1.8 mM  $\text{Ca}^{2+}$ , or both  $\text{Zn}^{2+}$  and  $\text{Ca}^{2+}$  Fig. 7B *left*), while the second aimed to examine the degree to which disruption of cytosolic  $\text{Zn}^{2+}$  buffering can exacerbate  $\text{Zn}^{2+}$ -triggered respiratory inhibition (via exposure to high  $\text{K}^+$ /MK-801 with 300  $\mu\text{M}$   $\text{Zn}^{2+}$ , 100  $\mu\text{M}$  DTDP alone, 10  $\mu\text{M}$   $\text{Zn}^{2+}$  + DTDP, all in 0  $\text{Ca}^{2+}$  HSS; Fig 7C *left*). When present, DTDP was added 10 min prior to, during and for 20 min after the high  $\text{K}^+$  exposures, to ensure strong disruption of buffering at the time of and for a period after the  $\text{Zn}^{2+}$  loading. Our findings were generally consistent with those above, examining  $\text{Zn}^{2+}$  effects on  $\psi_m$ , ROS generation, and mitochondrial morphology. Specifically, whereas OCR after high  $\text{K}^+$  exposures with either 300  $\mu\text{M}$   $\text{Zn}^{2+}$  or 1.8 mM  $\text{Ca}^{2+}$  alone was not different from that of control (wash into 1.8  $\text{Ca}^{2+}$  HSS), with combined  $\text{Zn}^{2+}$  and  $\text{Ca}^{2+}$  exposure, both the basal and the maximal uncoupled OCR (upon FCCP exposure) were substantially decreased (by  $\sim 50\%$ ) (Fig. 7B *right*). Similarly, whereas OCR after exposure to either 100  $\mu\text{M}$  DTDP or high  $\text{K}^+$ /300  $\mu\text{M}$   $\text{Zn}^{2+}$  alone was little different from that of control (wash into 0  $\text{Ca}^{2+}$  HSS), exposure to high  $\text{K}^+$ /10  $\mu\text{M}$   $\text{Zn}^{2+}$ /DTDP caused almost complete inhibition of respiration (Fig. 7C *right*). Of note, these effects on respiration were long-lasting, persisting even at the time of FCCP application ( $>2$  h after the high  $\text{K}^+$ / $\text{Zn}^{2+}$  exposures).

In sum, these findings further support the hypothesis that mitochondrial  $\text{Zn}^{2+}$  accumulation (enhanced and prolonged by disrupted cytosolic  $\text{Zn}^{2+}$  buffering), can act synergistically with  $\text{Ca}^{2+}$  to disrupt mitochondrial function. The intense swelling and long lasting respiratory inhibition caused by the low  $\text{Zn}^{2+}$  exposures with 100  $\mu\text{M}$  DTDP (but not by DTDP alone) lend further credence to the idea that  $\text{Zn}^{2+}$ -triggered mitochondrial dysfunction may be irreversible and contribute to neuronal death in pathological conditions.

### Mitochondrial $\text{Zn}^{2+}$ accumulation contributes to dose-dependent cell death

While above studies showing pronounced mitochondrial swelling and long lasting respiratory inhibition might predict that these effects would contribute to subsequent neurodegeneration, they are not in themselves indicative of cell death. We thus felt it important to carry out neurotoxicity studies, to more directly address the cytotoxic consequences of the mitochondrial effects (Fig. 8).

Two sets of studies—generally paralleling those on mitochondrial respiration (Fig. 7)—were carried out to assess the importance of both  $\text{Zn}^{2+}$ - $\text{Ca}^{2+}$  synergy and integrity of cytosolic  $\text{Zn}^{2+}$  buffering to delayed neurodegeneration. In the first set, cultures were exposed to high  $\text{K}^+$ /MK-801 with 300  $\mu\text{M}$   $\text{Zn}^{2+}$ , 1.8 mM  $\text{Ca}^{2+}$ , or both  $\text{Zn}^{2+}$  and  $\text{Ca}^{2+}$  for 5 min (Fig. 8A). In the second set, cultures were pre-exposed to 100  $\mu\text{M}$  DTDP prior to 5 min high  $\text{K}^+$ /MK-801 with 0, 50 or 100  $\mu\text{M}$   $\text{Zn}^{2+}$  ( $\pm \text{Ca}^{2+}$ ), followed by 10 min washout into DTDP (Fig. 8B). In both sets, neurons were transferred to MEM (supplemented with 25 mM glucose) and



returned to the incubator for 24 hrs after which neuronal injury was assessed via direct morphological examination and by lactate dehydrogenase (LDH) efflux assay (as described in Material and methods). Our findings are again consistent with above studies on mitochondrial function, with  $\text{Ca}^{2+}$  strongly enhancing  $\text{Zn}^{2+}$  triggered cell death (in neurons with both intact and disrupted buffering), and with  $\text{Zn}^{2+}$  exposure inducing dose-dependent injury under conditions of strongly disrupted buffering (Fig. 8A, B). While these findings do not directly prove that  $\text{Zn}^{2+}$  induced mitochondrial dysfunction caused the cell death, the similarity of effects for both mitochondrial dysfunction and neurodegeneration strongly suggest a link between the two.

In addition, to examine the temporal relationship between mitochondrial disruption and cell death (as indicated by LDH release, reflecting loss of membrane integrity), cultures were pre-exposed to 100  $\mu\text{M}$  DTDP prior to 5 min high  $\text{K}^+$ /MK-801 with 50  $\mu\text{M}$   $\text{Zn}^{2+}$  +  $\text{Ca}^{2+}$  followed by 10 min washout into DTDP (as in Fig. 8B), but with LDH release measured after both 2 hrs (when we observed near complete inhibition of respiration, see Fig. 7C) and after 24 hrs. We found the LDH release at 2 hrs to be less than half that at 24 hrs, highlighting the progressive cellular disintegration occurring after severe mitochondrial disruption (Fig. 8C).

If mitochondrial  $\text{Zn}^{2+}$  accumulation does contribute to neurodegeneration *in vivo* (such as after transient ischemia), it would be valuable to determine whether targeted delayed interventions could abrogate its effects, yielding better outcomes. To begin to address this possibility, we used the membrane permeable  $\text{Zn}^{2+}$  chelator TPEN. Cultures were subjected to an exposure we had found to cause rapid mitochondrial swelling and extensive neurodegeneration (high  $\text{K}^+$ /50  $\mu\text{M}$   $\text{Zn}^{2+}$ /100  $\mu\text{M}$  DTDP/MK-801 in 1.8  $\text{Ca}^{2+}$  HSS, with apocynin added in HET loaded cultures, as in Fig. 6, 8B). We first examined effects of this exposure on ROS generation, which can contribute to subsequent neuronal damage. This exposure caused a rapidly increasing HET F that persisted for at least 30 min after the 5 min  $\text{Zn}^{2+}$  exposure (much as in Fig. 5C). However, when TPEN (20  $\mu\text{M}$ ) was added immediately after washout of the high  $\text{K}^+$ / $\text{Zn}^{2+}$  exposure, the HET F was markedly attenuated (Fig. 9A). We then wondered whether this attenuation of ROS generation would be reflected by changes in subsequent neurodegeneration. To test this, cultures were exposed to high  $\text{K}^+$ /50  $\mu\text{M}$   $\text{Zn}^{2+}$ /100  $\mu\text{M}$  DTDP/MK-801 in 1.8  $\text{Ca}^{2+}$  HSS alone (as above; Fig. 8B) or with TPEN (10  $\mu\text{M}$ ) added either 10 min before, during and after the  $\text{Zn}^{2+}$  exposure (**TPEN pre-treatment**), or only after the  $\text{Zn}^{2+}$  exposure (**TPEN post-treatment**; Fig. 9B). While TPEN pre-treatment was markedly protective, validating the importance of  $\text{Zn}^{2+}$  to neuronal injury, it is notable that post-treatment was also modestly protective (Fig. 9B). As the effect of  $\text{Zn}^{2+}$  chelation on cell death parallels that on ROS generation (Fig. 9A), these findings further support the idea that mitochondrial dysfunction contributes to neurodegeneration and suggest the potential utility of delayed interventions. In sum, these findings not only strengthen the hypothesis that slow  $\text{Zn}^{2+}$  translocation via VSCC along with  $\text{Ca}^{2+}$ , under conditions of disrupted cytosolic  $\text{Zn}^{2+}$  buffering (as likely occurs during pathologic conditions), can induce mitochondrial dysfunction and cell death, but also suggest the exciting possibility that delayed modulation of mitochondrial  $\text{Zn}^{2+}$  accumulation could provide neuroprotection.



## Discussion

### Summary of findings

In the present study, we sought to elucidate effects of slow  $Zn^{2+}$  uptake via VSCC on mitochondrial function and subsequent neuronal injury. We find that with disrupted buffering, as likely occurs during *in vivo* ischemia, brief exposure to low  $Zn^{2+}$  under depolarizing conditions (to elicit extracellular  $Zn^{2+}$  entry through the VSCC) induced acute mitochondrial dysfunction, including loss of  $\Psi_m$ , ROS generation, mitochondrial swelling, and inhibition of respiration, as well as delayed neurodegeneration. The presence of physiologic levels of  $Ca^{2+}$  exacerbated these deleterious  $Zn^{2+}$  effects despite attenuating both cytosolic and mitochondrial  $Zn^{2+}$  accumulation, suggesting strong synergism between these ions. While our findings do not prove that  $Zn^{2+}$  triggered mitochondrial dysfunction directly led to neurodegeneration, the strong correlation between the effects of  $Zn^{2+}$  exposures under varied conditions on mitochondria with the induction of cell death supports the hypothesis that mitochondrial  $Zn^{2+}$  accumulation—and the consequent dysfunction—is an important upstream contributor to neuronal injury. Finally,  $Zn^{2+}$  chelation after  $Zn^{2+}$  loading attenuated both mitochondrial ROS generation and neuron death, further supporting the hypothesis that  $Zn^{2+}$  triggered mitochondrial dysfunction is an early contributor to neuronal damage, and that delayed, targeted interventions can be protective.

### $Zn^{2+}$ triggered neurodegeneration: ongoing questions about sources and targets

In light of the debilitating consequences of ischemic stroke, there is a compelling need to develop a better understanding of neuronal injury mechanism in order to identify neuroprotective targets. While attention has long focused on  $Ca^{2+}$  as the critical ionic contributor to neuronal injury, emerging clues—including observations of cytosolic  $Zn^{2+}$  accumulation in neurons after ischemia and findings that selective  $Zn^{2+}$  chelation can be neuroprotective—have highlighted important contribution of  $Zn^{2+}$  (Calderone et al., 2004; Koh et al., 1996; Tonder et al., 1990). Indeed, most  $Ca^{2+}$  indicators also respond to  $Zn^{2+}$  with greater affinity than  $Ca^{2+}$ , and it is likely that some effects previously attributed to  $Ca^{2+}$  are actually due to  $Zn^{2+}$  (Cheng and Reynolds, 1998; Stork and Li, 2006).

Our understanding of  $Zn^{2+}$  mechanisms in ischemia has been in flux. It was first assumed that the toxic  $Zn^{2+}$  accumulation seen after ischemia or prolonged seizures resulted from presynaptic release (Assaf and Chung, 1984; Howell et al., 1984) and its translocation into post-synaptic neurons (Koh et al., 1996; Tonder et al., 1990) through routes including VSCC and Ca-AMPA channels (Noh et al., 2005; Sensi et al., 2000; Yin et al., 2002). However, in studies using mice lacking presynaptic releasable  $Zn^{2+}$  (via knockout of the vesicular  $Zn^{2+}$  transporter, ZnT3) (Cole et al., 2000; Cole et al., 1999), prolonged seizures surprisingly still caused strong  $Zn^{2+}$  accumulation and  $Zn^{2+}$  dependent injury to CA1 pyramidal neurons, highlighting critical contributions from other sources (Lee et al., 2000). Further studies using ZnT3 knockouts as well as knockouts of the neuronal  $Zn^{2+}$  binding protein, metallothionein-III (MT-III) (Erickson et al., 1997), provided compelling evidence for distinct contributions of  $Zn^{2+}$  to neuronal injury between CA1 and CA3 pyramidal neurons, with  $Zn^{2+}$  translocation, likely in large part through Ca-AMPA channels, predominating in CA3, but mobilization from MT-III predominating in CA1 (Lee et al., 2000; Lee et al., 2003;

Medvedeva et al., 2017). Thus, it is now apparent that synaptically released  $Zn^{2+}$  as well as  $Zn^{2+}$  mobilized from intracellular binding proteins (like MT-III) can contribute to neuronal accumulation and injury in pathological conditions, although the respective contributions from these sources likely differ between populations of neurons.

Another unsettled question concerns the target(s) through which  $Zn^{2+}$  mediates injury. While it is apparent that  $Zn^{2+}$  can activate multiple pathways that contribute to neurodegeneration (Shuttleworth and Weiss, 2011), several lines of evidence led us to consider that mitochondria may be an important early target.  $Zn^{2+}$  has potent and complicated effects on isolated mitochondria, entering them through the mitochondrial  $Ca^{2+}$  uniporter (**MCU**), inhibiting electron transport and other critical mitochondrial enzymes at submicromolar concentrations, and triggering swelling via activation of mitochondrial permeability transition pore (**mPTP**); highlighting the complexity of these effects, they are exposure dependent, with low levels increasing respiration and inhibiting ROS production while high levels induced opposite effects (Brown et al., 2000; Dineley et al., 2005; Gazaryan et al., 2007; Jiang et al., 2001; Link and von Jagow, 1995; Sensi et al., 2003; Skulachev et al., 1967; Wudarczyk et al., 1999). In cultured neurons,  $Zn^{2+}$  loading via rapid entry through Ca-AMPA channels resulted in acute mitochondrial dysfunction, including rapid loss of  $\psi_m$  and ROS production (Sensi et al., 1999a; Sensi et al., 1999b, 2000), supporting the idea that mitochondria may be important  $Zn^{2+}$  targets in neuronal injury.

However, not all studies support this idea. First, brief fairly high (300  $\mu$ M)  $Zn^{2+}$  exposures to depolarized neurons (triggering slower  $Zn^{2+}$  translocation through VSCC) induced considerable delayed neurodegeneration but caused relatively little acute mitochondrial dysfunction (Pivovarova et al., 2014; Sensi et al., 1999a; Weiss et al., 1993). Furthermore, a recent study on isolated mitochondria in highly purified  $Ca^{2+}$  free buffer reported that in contrast to  $Ca^{2+}$ ,  $Zn^{2+}$  was a weak trigger of depolarization and did not trigger mPTP opening (Devinney et al., 2009). Thus, although  $Zn^{2+}$  appears to contribute to neurodegeneration after ischemia or prolonged seizures, there has been ongoing debate as to respective contributions of  $Zn^{2+}$  vs  $Ca^{2+}$  to mitochondrial dysfunction in these conditions.

### **Mitochondrial $Zn^{2+}$ accumulation and its consequences**

Despite evidence that both  $Zn^{2+}$  and  $Ca^{2+}$  contributed to neurodegeneration after ischemia or prolonged seizures, until recently there had been little attempt to discriminate their respective effects. To this aim, we carried out the first study seeking to track both ions simultaneously in single pyramidal neurons in hippocampal slices subjected to oxygen glucose deprivation (**OGD**) (Medvedeva et al., 2009), and found  $Zn^{2+}$  rises to precede and contribute to subsequent lethal  $Ca^{2+}$  overload; with  $Zn^{2+}$  chelation, the cell death was markedly delayed. Furthermore, the early  $Zn^{2+}$  effects appeared to depend upon its interaction with mitochondria (Medvedeva et al., 2009), with uptake of endogenous  $Zn^{2+}$  into mitochondria through the MCU contributing specifically to ROS production and neuronal cell death (Medvedeva and Weiss, 2014). Indeed, other studies have supported the idea that  $Zn^{2+}$  may contribute to mitochondrial dysfunction after *in vivo* ischemia, specifically promoting release of pro-apoptotic peptides from mitochondria and contributing

to the activation of large channels in the mitochondrial outer membranes (Bonanni et al., 2006; Calderone et al., 2004).

As noted above, despite some studies suggesting that  $Zn^{2+}$  may only weakly impact mitochondrial function (Devinney et al., 2009; Pivovarova et al., 2014), there has been a growing body of evidence that  $Zn^{2+}$ —as well as  $Ca^{2+}$ —can enter mitochondria and impact their function. While the nature of interactions between these ions on mitochondria has been little explored, prior studies have provided early clues for possible synergism between these ions. Specifically, combined application of  $Ca^{2+}$  and  $Zn^{2+}$  caused greater swelling of isolated mitochondria than  $Ca^{2+}$  or  $Zn^{2+}$  alone (Jiang et al., 2001), and  $Zn^{2+}$  entry through Ca-AMPA channels yielded stronger and more persistent ROS generation when  $Ca^{2+}$  was also present (Sensi et al., 2000). Present studies extend these early clues via examination of effects of slower  $Zn^{2+}$  and  $Ca^{2+}$  entry through VSCC, and find potent synergism between  $Zn^{2+}$  and  $Ca^{2+}$  on multiple measures of mitochondrial dysfunction. These findings are particularly notable, as brief  $Ca^{2+}$  influx through VSCC does not generally cause significant injury, and the presence of  $Ca^{2+}$  clearly resulted in a decreased amount of  $Zn^{2+}$  entering the neurons.

However, the nature of the interactions between  $Ca^{2+}$  and  $Zn^{2+}$  remains unclear and merits further study. One possibility is that the presence of  $Ca^{2+}$  may modify  $Zn^{2+}$  permeation through the MCU. While the MCU was previously considered to be quite selective for  $Ca^{2+}$ ,  $Zn^{2+}$  can also enter mitochondria through this route (Clausen et al., 2013; Gazaryan et al., 2007; Jiang et al., 2001; Malaiyandi et al., 2005; Saris and Niva, 1994), and  $Ca^{2+}$  was actually found to markedly facilitate  $Zn^{2+}$  entry through the MCU in isolated mitochondria (Saris and Niva, 1994). Studies of the recently identified MCU protein and associated regulatory peptides may yield further clues, with two peptides (termed MICU1 and MICU2) acting to regulate pore conductance as a function of the cytosolic  $Ca^{2+}$  concentration, inhibiting the channel when levels are low, and activating it when they rise (Kamer and Mootha, 2015; Marchi and Pinton, 2014; Murgia and Rizzuto, 2015). Thus, might some  $Ca^{2+}$  be needed for channel gating and  $Zn^{2+}$  entry, possibly accounting for the paucity of  $Zn^{2+}$  effects on isolated mitochondria carried out in purified  $Ca^{2+}$  free media (Devinney et al., 2009)? Indeed, a  $Ca^{2+}$  dependence for channel gating and  $Zn^{2+}$  entry through the MCU could contribute to the observed synergism between  $Ca^{2+}$  and  $Zn^{2+}$ .

The other unresolved issue concerns whether the levels of  $Zn^{2+}$  readily achieved in neurons in pathological conditions are likely to induce acute disruption of mitochondrial function, in light of observations (discussed above) that brief strong  $Zn^{2+}$  exposures to depolarized neurons caused little acute disruption of mitochondrial function (Pivovarova et al., 2014; Sensi et al., 1999a). However, although such relatively slow  $Zn^{2+}$  entry through VSCC does not cause the acute ROS production and strong loss of  $\Psi_m$  seen with more rapid entry (through Ca-AMPA channels), these exposures do result in persistent (at least 2 hrs)  $Zn^{2+}$  accumulation in mitochondria, contributing to partial loss of  $\Psi_m$  and release of pro-apoptotic peptides (Jiang et al., 2001; Sensi et al., 2002). It is also notable that strong disruption of cytosolic  $Zn^{2+}$  buffering alone (in the absence of extracellular  $Zn^{2+}$ ) results in sufficient intracellular  $Zn^{2+}$  mobilization to cause milder disruption of mitochondrial function and trigger delayed neurodegeneration (Aizenman et al., 2000; Bossy-Wetzel et al.,

2004; Sensi et al., 2003). Thus, perhaps it is not surprising that in combination, even relatively slow  $Zn^{2+}$  entry under conditions of impaired cytosolic  $Zn^{2+}$  buffering can acutely disrupt mitochondrial function.

In past studies we found that strong disruption of buffering enhanced ROS production caused by relatively low levels of  $Zn^{2+}$  entry (Clausen et al., 2013). Present studies markedly extend the understanding of conditions that determine effects of cellular  $Zn^{2+}$  loads on mitochondria. First, we find that even partial disruption of cytosolic  $Zn^{2+}$  buffering (that had little effect on its own), markedly increase mitochondrial dysfunction caused by brief  $Zn^{2+}$  exposures even at levels as low as 10  $\mu$ M. Secondly, we find that the effects are markedly enhanced by the presence of physiological levels of  $Ca^{2+}$  entry (and may be artificially inhibited under the non-physiological conditions of limited or absent  $Ca^{2+}$  in which many prior studies of  $Zn^{2+}$  were carried out). We further find that the enhanced disruption of mitochondria extends beyond the usual measures of loss of  $\Psi_m$  and ROS production to include strong and progressive swelling and long lasting inhibition of respiration, effects that may be indicative of severe or irrecoverable disruption. Finally, we examine effects of the presence of  $Ca^{2+}$  and disrupted  $Zn^{2+}$  buffering on cell death. While we do not definitively demonstrate that the  $Zn^{2+}$  dependent mitochondrial disruption leads directly to cell death, we found the effects on mitochondrial function to be strongly correlated with those on cell death and that delayed  $Zn^{2+}$  chelation attenuated both the mitochondrial ROS generation and the subsequent neurodegeneration. Thus, our studies provide new support to the idea that  $Zn^{2+}$  triggered mitochondrial disruption is an important upstream event that contributes to delayed injury, the targeting of which could be protective.

### Conclusions and possible therapeutic implications

We started with the comment that the available treatments for ischemia injury are inadequate, reflecting in part incomplete understanding of relevant targetable events. We wish to end by suggesting a new hypothesis: *Early mitochondrial  $Zn^{2+}$  accumulation—and the consequent disruption of their function—is a critical and targetable event in the neurodegenerative sequence.* The validity of this hypothesis depends upon a number of factors: **1.** The occurrence of disrupted buffering. It is apparent that acidosis and oxidative stress occur in the context of ischemia, and can result in the disruption of cytosolic  $Zn^{2+}$  buffering and its toxic accumulation in neurons (Aizenman et al., 2000; Lee et al., 2000; Sensi et al., 2003; Shuttleworth and Weiss, 2011; Weiss et al., 2000). **2.** The occurrence of  $Zn^{2+}$  accumulation in the extracellular space. It is difficult to accurately quantify  $Zn^{2+}$  accumulation in brain resulting from synaptic release; early estimates that peak levels reach 100–300  $\mu$ M (Frederickson, 1989) are probably high. Widespread extracellular accumulation with ischemia or seizures certainly occurs, and recent studies suggest that levels in the 10–100  $\mu$ M range may be achievable in areas of hippocampus and cortex where there is considerable synaptic  $Zn^{2+}$  (Frederickson et al., 2006; Ueno et al., 2002; Vogt et al., 2000). Although neurons expressing Ca-AMPA channels may get the strongest  $Zn^{2+}$  loads, present studies suggest that even brief presence of as little as 10  $\mu$ M  $Zn^{2+}$  may result in sufficient entry into any depolarized neurons with impaired cytosolic  $Zn^{2+}$  buffering to trigger acute mitochondrial disruption. In light of observations that VSCC activity increases with aging and chronic hypoxia (Thibault and Landfield 1996, Campbell et al 1996, Webster et al

2006), these effects may be greater still in the aging populations most at risk of ischemic attack.

Present studies also provide a “proof of principle” for the potential utility of delayed delivery of  $Zn^{2+}$  targeting interventions – with  $Zn^{2+}$  chelation after the  $Zn^{2+}$  exposure decreasing both ROS generation and subsequent cell death (Fig. 9), consistent with other recent findings on OGD induced ROS production (Slepchenko et al., 2017). Optimal interventions may vary depending on when the intervention is delivered. In the early phases, interventions targeting  $Zn^{2+}$  entry into mitochondria might include  $Zn^{2+}$  chelators, MCU blockers, or antioxidants (to diminish oxidative disruption of buffering) while at later stages, mPTP blockers may decrease mitochondrial swelling and mediator release (Friberg and Wieloch, 2002). Of note, most drugs have multiple effects complicating the development of optimal interventions. For instance, whereas MCU blockers alone in early stages of ischemia might diminish mitochondrial  $Zn^{2+}$  accumulation, they could hasten injury by promoting cytosolic  $Ca^{2+}$  overload (Medvedeva and Weiss, 2014; Velasco and Tapia, 2000).

We further suggest that consequences of mitochondrial  $Zn^{2+}$  loading are variable; with very strong loads resulting in acute irreversible mitochondrial disruption and cell death (Medvedeva et al., 2009; Medvedeva and Weiss, 2014), while milder ischemia may result in alterations in mitochondrial function that may contribute to the activation of downstream delayed cell death pathways. Recent findings are compatible with this idea. CA1 pyramidal neurons undergo selective delayed degeneration after transient ischemia, which is associated with delayed mitochondrial swelling and cytochrome C release (Sugawara et al., 1999). Interestingly, in recent slice studies, we found persistent  $Zn^{2+}$  accumulation in CA1 mitochondria after transient sublethal OGD (Medvedeva et al., 2017). In light of the demonstrated potent ability of mitochondrial  $Zn^{2+}$  to trigger dysfunction including ROS generation, swelling, mPTP activation and cytochrome C release (Gazaryan et al., 2007; Jiang et al., 2001; Weiss et al., 2000) might the  $Zn^{2+}$  be a targetable trigger for the downstream death promoting events? One such mechanism may be the delayed insertion of Kv2.1  $K^+$  channels that can cause a form of apoptotic neurodegeneration (Aizenman et al., 2000; McLaughlin et al., 2001). As mitochondrial ROS has been implicated in the activation of both p38 mitogen-activated protein kinase (MAPK) and apoptosis signal-regulating kinase 1 (ASK1) (Bossy-Wetzel et al., 2004; Soberanes et al., 2009), both of which are essential for insertion of the Kv2.1  $K^+$  channels (Aras and Aizenman, 2005; McLaughlin et al., 2001), perhaps  $Zn^{2+}$  induced mitochondrial dysfunction is a critical upstream contributor to these events? In sum, we feel that considerable data—including findings from present study—highlights the likely importance of early interactions of  $Zn^{2+}$  with mitochondria as a trigger of acute and delayed injury after brain ischemia or prolonged seizures, and that efforts to target these early events could yield therapeutic benefits.

## Acknowledgments

Supported by NIH grants NS065219 and NS096987 (JHW), and a grant from the American Heart Association (JHW). The authors declare no competing financial interests.

## Abbreviations

<b>AMPA</b>	$\alpha$ -amino-3-hydroxy-5-methyl-4-isoxazolepropionic acid
<b>Ca-AMPA</b>	Ca <sup>2+</sup> permeable AMPA channels
<b>FCCP</b>	carbonyl cyanide-p-trifluoromethoxyphenylhydrazone
<b>DTDP</b>	2,2'-dithiodipyridine
<b>HEt</b>	hydroethidine
<b>MT</b>	metallothionein
<b>NMDA</b>	N-methyl-D-aspartate
<b>TPEN</b>	N,N,N,N-tetrakis(2-pyridylmethyl)ethane-1,2-diamine
<b>OGD</b>	oxygen glucose deprivation
<b>ROS</b>	reactive oxygen species
<b>Rhod123</b>	rhodamine 123
<b>VSCC</b>	voltage sensitive Ca <sup>2+</sup> channels

## References

- Aizenman E, Stout AK, Hartnett KA, Dineley KE, McLaughlin B, Reynolds IJ. Induction of neuronal apoptosis by thiol oxidation: putative role of intracellular zinc release. *J Neurochem.* 2000; 75:1878–1888. [PubMed: 11032877]
- Aras MA, Aizenman E. Obligatory role of ASK1 in the apoptotic surge of K<sup>+</sup> currents. *Neurosci Lett.* 2005; 387:136–140. [PubMed: 16006035]
- Assaf SY, Chung SH. Release of endogenous Zn<sup>2+</sup> from brain tissue during activity. *Nature.* 1984; 308:734–736. [PubMed: 6717566]
- Bindokas VP, Jordan J, Lee CC, Miller RJ. Superoxide production in rat hippocampal neurons: selective imaging with hydroethidine. *J Neurosci.* 1996; 16:1324–1336. [PubMed: 8778284]
- Bonanni L, Chachar M, Jover-Mengual T, Li H, Jones A, Yokota H, Ofengeim D, Flannery RJ, Miyawaki T, Cho CH, Polster BM, Pypaert M, Hardwick JM, Sensi SL, Zukin RS, Jonas EA. Zinc-dependent multi-conductance channel activity in mitochondria isolated from ischemic brain. *J Neurosci.* 2006; 26:6851–6862. [PubMed: 16793892]
- Bossy-Wetzell E, Talantova MV, Lee WD, Scholzke MN, Harrop A, Mathews E, Gotz T, Han J, Ellisman MH, Perkins GA, Lipton SA. Crosstalk between Nitric Oxide and Zinc Pathways to Neuronal Cell Death Involving Mitochondrial Dysfunction and p38-Activated K(+) Channels. *Neuron.* 2004; 41:351–365. [PubMed: 14766175]
- Brand MD, Nicholls DG. Assessing mitochondrial dysfunction in cells. *The Biochemical journal.* 2011; 435:297–312. [PubMed: 21726199]
- Brennan AM, Suh SW, Won SJ, Narasimhan P, Kauppinen TM, Lee H, Edling Y, Chan PH, Swanson RA. NADPH oxidase is the primary source of superoxide induced by NMDA receptor activation. *Nature neuroscience.* 2009; 12:857–863. [PubMed: 19503084]
- Brown AM, Kristal BS, Effron MS, Shestopalov AI, Ullucci PA, Sheu KF, Blass JP, Cooper AJ. Zn<sup>2+</sup> inhibits alpha-ketoglutarate-stimulated mitochondrial respiration and the isolated alpha-ketoglutarate dehydrogenase complex. *J Biol Chem.* 2000; 275:13441–13447. [PubMed: 10788456]



- Brustovetsky N, Brustovetsky T, Jemmerson R, Dubinsky JM. Calcium-induced cytochrome c release from CNS mitochondria is associated with the permeability transition and rupture of the outer membrane. *J Neurochem.* 2002; 80:207–218. [PubMed: 11902111]
- Buckman JF, Hernandez H, Kress GJ, Votyakova TV, Pal S, Reynolds IJ. MitoTracker labeling in primary neuronal and astrocytic cultures: influence of mitochondrial membrane potential and oxidants. *Journal of neuroscience methods.* 2001; 104:165–176. [PubMed: 11164242]
- Calderone A, Jover T, Mashiko T, Noh KM, Tanaka H, Bennett MV, Zukin RS. Late calcium EDTA rescues hippocampal CA1 neurons from global ischemia-induced death. *J Neurosci.* 2004; 24:9903–9913. [PubMed: 15525775]
- Campbell LW, Hao SY, Thibault O, Blalock EM, Landfield PW. Aging changes in voltage-gated calcium currents in hippocampal CA1 neurons. *J Neurosci.* 1996; 16:6286–6295. [PubMed: 8815908]
- Canzoniero LM, Turetsky DM, Choi DW. Measurement of intracellular free zinc concentrations accompanying zinc-induced neuronal death. *J Neurosci.* 1999; 19:RC31. [PubMed: 10493776]
- Cheng C, Reynolds IJ. Calcium-sensitive fluorescent dyes can report increases in intracellular free zinc concentration in cultured forebrain neurons. *J Neurochem.* 1998; 71:2401–2410. [PubMed: 9832138]
- Choi DW, Koh JY, Peters S. Pharmacology of glutamate neurotoxicity in cortical cell culture: attenuation by NMDA antagonists. *J Neurosci.* 1988; 8:185–196. [PubMed: 2892896]
- Clausen A, McClanahan T, Ji SG, Weiss JH. Mechanisms of Rapid Reactive Oxygen Species Generation in response to Cytosolic Ca<sup>2+</sup> or Zn<sup>2+</sup> Loads in Cortical Neurons. *Plos One.* 2013; 8:e83347. [PubMed: 24340096]
- Cole TB, Robbins CA, Wenzel HJ, Schwartzkroin PA, Palmiter RD. Seizures and neuronal damage in mice lacking vesicular zinc. *Epilepsy Res.* 2000; 39:153–169. [PubMed: 10759303]
- Cole TB, Wenzel HJ, Kafer KE, Schwartzkroin PA, Palmiter RD. Elimination of zinc from synaptic vesicles in the intact mouse brain by disruption of the ZnT3 gene. *Proc Natl Acad Sci U S A.* 1999; 96:1716–1721. [PubMed: 9990090]
- Colvin RA, Holmes WR, Fontaine CP, Maret W. Cytosolic zinc buffering and muffling: their role in intracellular zinc homeostasis. *Metallomics: integrated biometal science.* 2010; 2:306–317. [PubMed: 21069178]
- Devinney MJ, Malaiyandi LM, Vergun O, DeFranco DB, Hastings TG, Dineley KE. A comparison of Zn<sup>2+</sup>- and Ca<sup>2+</sup>-triggered depolarization of liver mitochondria reveals no evidence of Zn<sup>2+</sup>-induced permeability transition. *Cell calcium.* 2009; 45:447–455. [PubMed: 19349076]
- Dineley KE, Richards LL, Votyakova TV, Reynolds IJ. Zinc causes loss of membrane potential and elevates reactive oxygen species in rat brain mitochondria. *Mitochondrion.* 2005; 5:55–65. [PubMed: 16060292]
- Duchen MR, Surin A, Jacobson J. Imaging mitochondrial function in intact cells. *Methods in enzymology.* 2003; 361:353–389. [PubMed: 12624920]
- Erickson JC, Hollopeter G, Thomas SA, Froelick GJ, Palmiter RD. Disruption of the metallothionein-III gene in mice: analysis of brain zinc, behavior, and neuron vulnerability to metals, aging, and seizures. *J Neurosci.* 1997; 17:1271–1281. [PubMed: 9006971]
- Frederickson CJ. Neurobiology of zinc and zinc-containing neurons. *Int Rev Neurobiol.* 1989; 31:145–238. [PubMed: 2689380]
- Frederickson CJ, Giblin LJ, Krezel A, McAdoo DJ, Mueller RN, Zeng Y, Balaji RV, Masalha R, Thompson RB, Fierke CA, Sarvey JM, de Valdenbro M, Prough DS, Zornow MH. Concentrations of extracellular free zinc (pZn)<sub>e</sub> in the central nervous system during simple anesthetization, ischemia and reperfusion. *Exp Neurol.* 2006; 198:285–293. [PubMed: 16443223]
- Frederickson CJ, Hernandez MD, McGinty JF. Translocation of zinc may contribute to seizure-induced death of neurons. *Brain Res.* 1989; 480:317–321. [PubMed: 2713657]
- Frederickson CJ, Koh JY, Bush AI. The neurobiology of zinc in health and disease. *Nature reviews Neuroscience.* 2005; 6:449–462. [PubMed: 15891778]
- Friberg H, Wieloch T. Mitochondrial permeability transition in acute neurodegeneration. *Biochimie.* 2002; 84:241–250. [PubMed: 12022955]



- Gazaryan IG, Krasinskaya IP, Kristal BS, Brown AM. Zinc irreversibly damages major enzymes of energy production and antioxidant defense prior to mitochondrial permeability transition. *J Biol Chem.* 2007; 282:24373–24380. [PubMed: 17565998]
- Gee KR, Zhou ZL, Ton-That D, Sensi SL, Weiss JH. Measuring zinc in living cells. A new generation of sensitive and selective fluorescent probes. *Cell calcium.* 2002; 31:245–251. [PubMed: 12098227]
- Halestrap AP. Calcium, mitochondria and reperfusion injury: a pore way to die. *Biochemical Society transactions.* 2006; 34:232–237. [PubMed: 16545083]
- Howell GA, Welch MG, Frederickson CJ. Stimulation-induced uptake and release of zinc in hippocampal slices. *Nature.* 1984; 308:736–738. [PubMed: 6717567]
- Hoyte L, Barber PA, Buchan AM, Hill MD. The rise and fall of NMDA antagonists for ischemic stroke. *Current molecular medicine.* 2004; 4:131–136. [PubMed: 15032709]
- Ikonomidou C, Turski L. Why did NMDA receptor antagonists fail clinical trials for stroke and traumatic brain injury? *The Lancet. Neurology.* 2002; 1:383–386. [PubMed: 12849400]
- Jia Y, Jeng JM, Sensi SL, Weiss JH. Zn<sup>2+</sup> currents are mediated by calcium-permeable AMPA/kainate channels in cultured murine hippocampal neurones. *J Physiol.* 2002; 543:35–48. [PubMed: 12181280]
- Jiang D, Sullivan PG, Sensi SL, Steward O, Weiss JH. Zn(2+) induces permeability transition pore opening and release of pro-apoptotic peptides from neuronal mitochondria. *J Biol Chem.* 2001; 276:47524–47529. [PubMed: 11595748]
- Kamer KJ, Mootha VK. The molecular era of the mitochondrial calcium uniporter. *Nature reviews Molecular cell biology.* 2015; 16:545–553. [PubMed: 26285678]
- Kerchner GA, Canzoniero LM, Yu SP, Ling C, Choi DW. Zn<sup>2+</sup> current is mediated by voltage-gated Ca<sup>2+</sup> channels and enhanced by extracellular acidity in mouse cortical neurones. *J Physiol.* 2000; 528(Pt 1):39–52. [PubMed: 11018104]
- Koh JY, Choi DW. Quantitative determination of glutamate mediated cortical neuronal injury in cell culture by lactate dehydrogenase efflux assay. *Journal of neuroscience methods.* 1987; 20:83–90. [PubMed: 2884353]
- Koh JY, Suh SW, Gwag BJ, He YY, Hsu CY, Choi DW. The role of zinc in selective neuronal death after transient global cerebral ischemia. *Science.* 1996; 272:1013–1016. [PubMed: 8638123]
- Lee JY, Cole TB, Palmiter RD, Koh JY. Accumulation of zinc in degenerating hippocampal neurons of ZnT3-null mice after seizures: evidence against synaptic vesicle origin. *J Neurosci.* 2000; 20:RC79. [PubMed: 10807937]
- Lee JY, Kim JH, Palmiter RD, Koh JY. Zinc released from metallothionein-iii may contribute to hippocampal CA1 and thalamic neuronal death following acute brain injury. *Exp Neurol.* 2003; 184:337–347. [PubMed: 14637104]
- Link TA, von Jagow G. Zinc ions inhibit the QP center of bovine heart mitochondrial bc1 complex by blocking a protonatable group. *J Biol Chem.* 1995; 270:25001–25006. [PubMed: 7559629]
- Malaiyandi LM, Dineley KE, Reynolds IJ. Divergent consequences arise from metallothionein overexpression in astrocytes: zinc buffering and oxidant-induced zinc release. *Glia.* 2004; 45:346–353. [PubMed: 14966866]
- Malaiyandi LM, Vergun O, Dineley KE, Reynolds IJ. Direct visualization of mitochondrial zinc accumulation reveals uniporter-dependent and -independent transport mechanisms. *J Neurochem.* 2005; 93:1242–1250. [PubMed: 15934944]
- Marchi S, Pinton P. The mitochondrial calcium uniporter complex: molecular components, structure and pathophysiological implications. *J Physiol.* 2014; 592:829–839. [PubMed: 24366263]
- Maret W. Redox biochemistry of mammalian metallothioneins. *Journal of biological inorganic chemistry: JBIC: a publication of the Society of Biological Inorganic Chemistry.* 2011; 16:1079–1086. [PubMed: 21647775]
- Maret W. Analyzing free zinc(II) ion concentrations in cell biology with fluorescent chelating molecules. *Metallomics: integrated biometal science.* 2015; 7:202–211. [PubMed: 25362967]
- Maret W, Vallee BL. Thiolate ligands in metallothionein confer redox activity on zinc clusters. *Proc Natl Acad Sci U S A.* 1998; 95:3478–3482. [PubMed: 9520391]

- McCord MC, Aizenman E. Convergent Ca<sup>2+</sup> and Zn<sup>2+</sup> signaling regulates apoptotic Kv2.1 K<sup>+</sup> currents. *Proc Natl Acad Sci U S A*. 2013; 110:13988–13993. [PubMed: 23918396]
- McLaughlin B, Pal S, Tran MP, Parsons AA, Barone FC, Erhardt JA, Aizenman E. p38 activation is required upstream of potassium current enhancement and caspase cleavage in thiol oxidant-induced neuronal apoptosis. *J Neurosci*. 2001; 21:3303–3311. [PubMed: 11331359]
- Medvedeva YV, Ji SG, Yin HZ, Weiss JH. Differential Vulnerability of CA1 versus CA3 Pyramidal Neurons After Ischemia: Possible Relationship to Sources of Zn<sup>2+</sup> Accumulation and Its Entry into and Prolonged Effects on Mitochondria. *J Neurosci*. 2017; 37:726–737. [PubMed: 28100752]
- Medvedeva YV, Lin B, Shuttleworth CW, Weiss JH. Intracellular Zn<sup>2+</sup> accumulation contributes to synaptic failure, mitochondrial depolarization, and cell death in an acute slice oxygen-glucose deprivation model of ischemia. *J Neurosci*. 2009; 29:1105–1114. [PubMed: 19176819]
- Medvedeva YV, Weiss JH. Intramitochondrial Zn(2+) accumulation via the Ca(2+) uniporter contributes to acute ischemic neurodegeneration. *Neurobiology of disease*. 2014; 68:137–144. [PubMed: 24787898]
- Murgia M, Rizzuto R. Molecular diversity and pleiotropic role of the mitochondrial calcium uniporter. *Cell calcium*. 2015; 58:11–17. [PubMed: 26048007]
- Nicholls DG, Budd SL. Mitochondria and neuronal survival. *Physiol Rev*. 2000; 80:315–360. [PubMed: 10617771]
- Noh KM, Koh JY. Induction and activation by zinc of NADPH oxidase in cultured cortical neurons and astrocytes. *J Neurosci*. 2000; 20:RC111. [PubMed: 11090611]
- Noh KM, Yokota H, Mashiko T, Castillo PE, Zukin RS, Bennett MV. Blockade of calcium-permeable AMPA receptors protects hippocampal neurons against global ischemia-induced death. *Proc Natl Acad Sci U S A*. 2005; 102:12230–12235. [PubMed: 16093311]
- Pivovarova NB, Stanika RI, Kazanina G, Villanueva I, Andrews SB. The interactive roles of zinc and calcium in mitochondrial dysfunction and neurodegeneration. *J Neurochem*. 2014; 128:592–602. [PubMed: 24127746]
- Rothman SM, Olney JW. Glutamate and the pathophysiology of hypoxic--ischemic brain damage. *Ann Neurol*. 1986; 19:105–111. [PubMed: 2421636]
- Saris NE, Niva K. Is Zn<sup>2+</sup> transported by the mitochondrial calcium uniporter? *FEBS Lett*. 1994; 356:195–198. [PubMed: 7528685]
- Sensi SL, Ton-That D, Sullivan PG, Jonas EA, Gee KR, Kaczmarek LK, Weiss JH. Modulation of mitochondrial function by endogenous Zn<sup>2+</sup> pools. *Proc Natl Acad Sci U S A*. 2003; 100:6157–6162. [PubMed: 12724524]
- Sensi SL, Ton-That D, Weiss JH. Mitochondrial sequestration and Ca(2+)-dependent release of cytosolic Zn(2+) loads in cortical neurons. *Neurobiology of disease*. 2002; 10:100–108. [PubMed: 12127148]
- Sensi SL, Yin HZ, Carriedo SG, Rao SS, Weiss JH. Preferential Zn<sup>2+</sup> influx through Ca<sup>2+</sup>-permeable AMPA/kainate channels triggers prolonged mitochondrial superoxide production. *Proc Natl Acad Sci U S A*. 1999a; 96:2414–2419. [PubMed: 10051656]
- Sensi SL, Yin HZ, Weiss JH. Glutamate triggers preferential Zn<sup>2+</sup> flux through Ca<sup>2+</sup> permeable AMPA channels and consequent ROS production. *Neuroreport*. 1999b; 10:1723–1727. [PubMed: 10501564]
- Sensi SL, Yin HZ, Weiss JH. AMPA/kainate receptor-triggered Zn<sup>2+</sup> entry into cortical neurons induces mitochondrial Zn<sup>2+</sup> uptake and persistent mitochondrial dysfunction. *The European journal of neuroscience*. 2000; 12:3813–3818. [PubMed: 11029652]
- Shuttleworth CW, Weiss JH. Zinc: new clues to diverse roles in brain ischemia. *Trends Pharmacol Sci*. 2011; 32:480–486. [PubMed: 21621864]
- Skulachev VP, Chistyakov VV, Jasaitis AA, Smirnova EG. Inhibition of the respiratory chain by zinc ions. *Biochemical and biophysical research communications*. 1967; 26:1–6. [PubMed: 4291553]
- Slepchenko KG, Lu Q, Li YV. Cross talk between increased intracellular zinc (Zn<sup>2+</sup>) and accumulation of reactive oxygen species in chemical ischemia. *American journal of physiology Cell physiology*. 2017; 313:C448–C459. [PubMed: 28747335]
- Soberanes S, Urlich D, Baker CM, Burgess Z, Chiarella SE, Bell EL, Ghio AJ, De Vizcaya-Ruiz A, Liu J, Ridge KM, Kamp DW, Chandel NS, Schumacker PT, Mutlu GM, Budinger GR. Mitochondrial

complex III-generated oxidants activate ASK1 and JNK to induce alveolar epithelial cell death following exposure to particulate matter air pollution. *J Biol Chem.* 2009; 284:2176–2186. [PubMed: 19033436]

- Stork CJ, Li YV. Intracellular zinc elevation measured with a “calcium-specific” indicator during ischemia and reperfusion in rat hippocampus: a question on calcium overload. *J Neurosci.* 2006; 26:10430–10437. [PubMed: 17035527]
- Sugawara T, Fujimura M, Morita-Fujimura Y, Kawase M, Chan PH. Mitochondrial release of cytochrome c corresponds to the selective vulnerability of hippocampal CA1 neurons in rats after transient global cerebral ischemia. *J Neurosci.* 1999; 19:RC39. [PubMed: 10559429]
- Thibault O, Landfield PW. Increase in single L-type calcium channels in hippocampal neurons during aging. *Science.* 1996; 272:1017–1020. [PubMed: 8638124]
- Tonder N, Johansen FF, Frederickson CJ, Zimmer J, Diemer NH. Possible role of zinc in the selective degeneration of dentate hilar neurons after cerebral ischemia in the adult rat. *Neurosci Lett.* 1990; 109:247–252. [PubMed: 2330128]
- Ueno S, Tsukamoto M, Hirano T, Kikuchi K, Yamada MK, Nishiyama N, Nagano T, Matsuki N, Ikegaya Y. Mossy fiber Zn<sup>2+</sup> spillover modulates heterosynaptic N-methyl-D-aspartate receptor activity in hippocampal CA3 circuits. *The Journal of cell biology.* 2002; 158:215–220. [PubMed: 12119362]
- Velasco I, Tapia R. Alterations of intracellular calcium homeostasis and mitochondrial function are involved in ruthenium red neurotoxicity in primary cortical cultures. *Journal of neuroscience research.* 2000; 60:543–551. [PubMed: 10797557]
- Vogt K, Mellor J, Tong G, Nicoll R. The actions of synaptically released zinc at hippocampal mossy fiber synapses. *Neuron.* 2000; 26:187–196. [PubMed: 10798403]
- Webster NJ, Ramsden M, Boyle JP, Pearson HA, Peers C. Amyloid peptides mediate hypoxic increase of L-type Ca<sup>2+</sup> channels in central neurones. *Neurobiol Aging.* 2006; 27:439–445. [PubMed: 16464656]
- Weiss JH, Hartley DM, Koh JY, Choi DW. AMPA receptor activation potentiates zinc neurotoxicity. *Neuron.* 1993; 10:43–49. [PubMed: 7678965]
- Weiss JH, Sensi SL, Koh JY. Zn(2+): a novel ionic mediator of neural injury in brain disease. *Trends Pharmacol Sci.* 2000; 21:395–401. [PubMed: 11050320]
- Wudarczyk J, Debska G, Lenartowicz E. Zinc as an inducer of the membrane permeability transition in rat liver mitochondria. *Archives of biochemistry and biophysics.* 1999; 363:1–8. [PubMed: 10049493]
- Yao J, Irwin RW, Zhao L, Nilsen J, Hamilton RT, Brinton RD. Mitochondrial bioenergetic deficit precedes Alzheimer’s pathology in female mouse model of Alzheimer’s disease. *Proc Natl Acad Sci U S A.* 2009; 106:14670–14675. [PubMed: 19667196]
- Yin H, Turetsky D, Choi DW, Weiss JH. Cortical neurones with Ca<sup>2+</sup> permeable AMPA/kainate channels display distinct receptor immunoreactivity and are GABAergic. *Neurobiology of disease.* 1994; 1:43–49. [PubMed: 9216985]
- Yin HZ, Sensi SL, Ogoshi F, Weiss JH. Blockade of Ca<sup>2+</sup>-permeable AMPA/kainate channels decreases oxygen-glucose deprivation-induced Zn<sup>2+</sup> accumulation and neuronal loss in hippocampal pyramidal neurons. *J Neurosci.* 2002; 22:1273–1279. [PubMed: 11850455]
- Yin HZ, Weiss JH. Zn(2+) permeates Ca(2+) permeable AMPA/kainate channels and triggers selective neural injury. *Neuroreport.* 1995; 6:2553–2556. [PubMed: 8741761]

### Highlights

- Excitotoxic  $Zn^{2+}$  and/or  $Ca^{2+}$  accumulation can trigger neuronal injury in vitro
- Slow neuronal  $Zn^{2+}$  entry causes mitochondrial uptake and mild functional disruption
- These effects are markedly increased upon disruption of cytosolic  $Zn^{2+}$  buffering
- $Ca^{2+}$  impedes neuronal  $Zn^{2+}$  entry but markedly enhances its impact on mitochondria
- Mitochondrial  $Zn^{2+}$  accumulation may be a viable target for neuroprotection

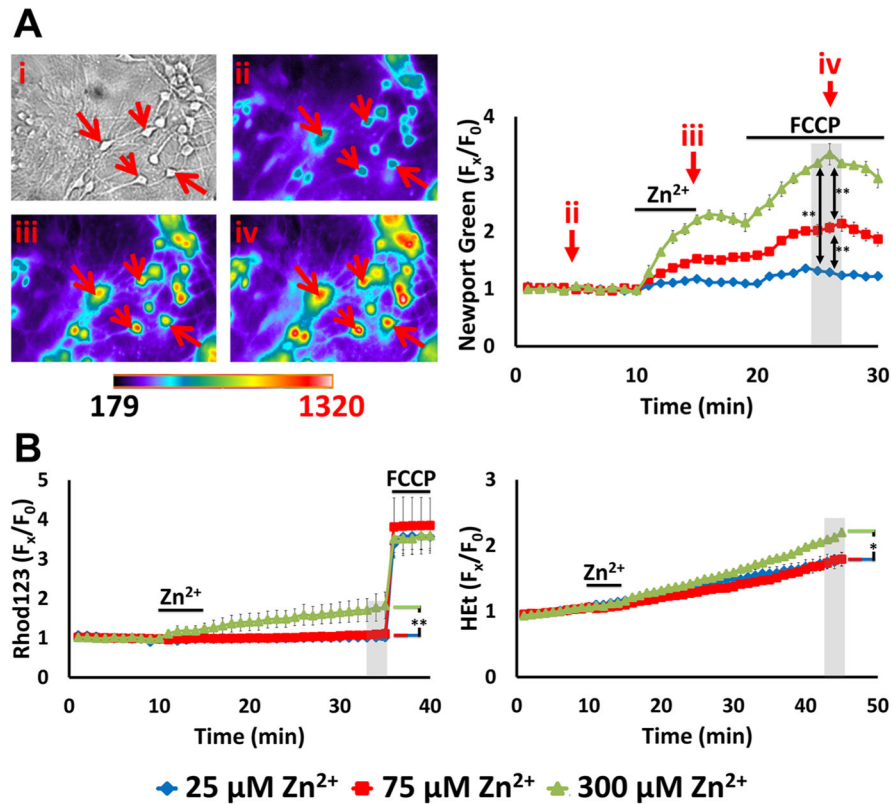


**Figure 1. High  $\text{K}^+/\text{Zn}^{2+}$  exposures induce dose-dependent mitochondrial  $\text{Zn}^{2+}$  uptake but only mild acute dysfunction**

**A. High  $\text{K}^+/\text{Zn}^{2+}$  exposures cause dose-dependent mitochondrial  $\text{Zn}^{2+}$  accumulation.**

Cultures were loaded with the low affinity cytosolic  $\text{Zn}^{2+}$  indicator Newport Green ( $K_d \sim 1 \mu\text{M}$ ), exposed to 90 mM  $\text{K}^+$  (high  $\text{K}^+$ ) with  $\text{Zn}^{2+}$  (25, 75, 300  $\mu\text{M}$ ) for 5 min in 0  $\text{Ca}^{2+}$  HSS, followed by wash into 0  $\text{Ca}^{2+}$  HSS for additional 5 min prior to application of FCCP (1  $\mu\text{M}$ ).

**Left:** Representative images: Brightfield image (i) shows appearance of neurons at baseline, and pseudocolor images show Newport Green fluorescence from the same field at baseline (ii), 5 min after high  $\text{K}^+/\text{300 } \mu\text{M Zn}^{2+}$  exposure (iii), and 5 min after FCCP (iv). (Arrows highlight the same neurons in these images.) **Right:** Traces show time course of Newport Green  $F$  (background subtracted and normalized to baseline [ $F_x/F_0$ ]; arrows indicate the time points illustrated in the images), and represent means  $\pm$  standard error of the mean (SEM) of 6 experiments, 120 neurons. Grey bar indicates time points of comparison (\*\* indicates  $p < 0.01$  by one-way ANOVA with Tukey post hoc). Note the  $\text{Zn}^{2+}$  exposure concentration-dependent mitochondrial  $\text{Zn}^{2+}$  accumulation, indicated by the increase in  $F$  after FCCP

**B). These exposures only induce mild mitochondrial dysfunction:** Cultures were loaded with the  $\Psi_{\text{mito}}$  sensitive indicator, Rhod123, or the superoxide preferring ROS indicator, HET, and exposed to high  $\text{K}^+/\text{Zn}^{2+}$  for 5 min, followed by wash into 0  $\text{Ca}^{2+}$  HSS, as above. After 20 min, FCCP (1  $\mu\text{M}$ ) was applied to Rhod123-loaded cultures to induce full loss of  $\Psi_{\text{m}}$ . Traces show time course of Rhod123  $F$  (left) or HET  $F$  (right), normalized to baseline values (after background subtraction, as above;  $F_x/F_0$ ), and represent mean  $\pm$  SEM 6 experiments, 120 neurons. Grey bars indicate time points of comparison (\* indicates  $p <$

0.05, \*\* indicates  $p < 0.01$ , by one-way ANOVA with Tukey post hoc). Note that only 300  $\mu\text{M Zn}^{2+}$  exposure induced discernable effects.

Author Manuscript

Author Manuscript

Author Manuscript

Author Manuscript

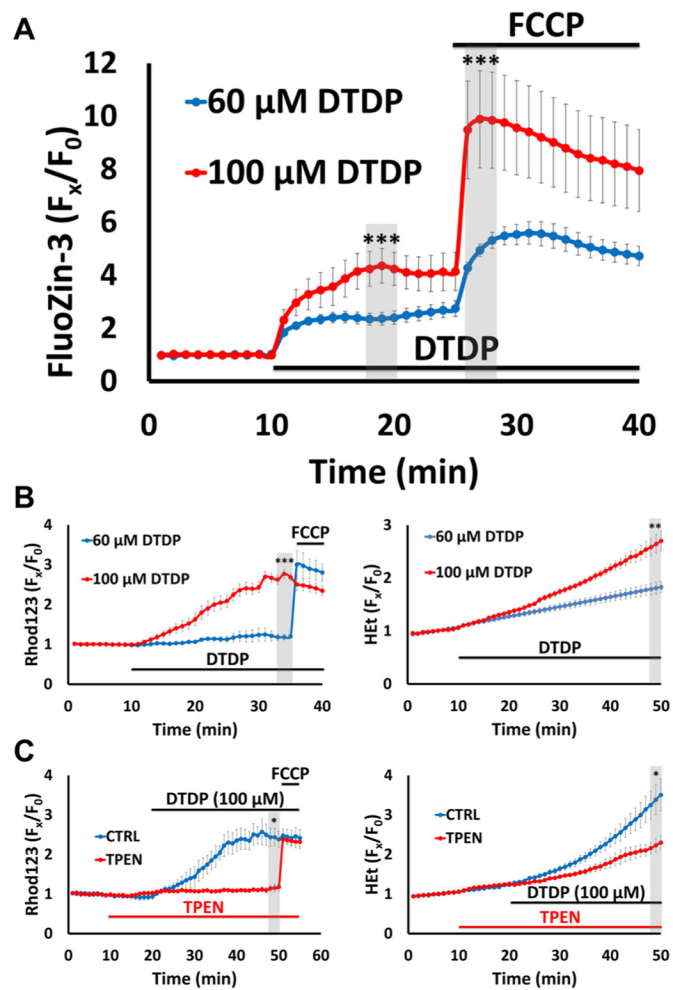


### Figure 2. Disruption of cytosolic $Zn^{2+}$ buffering leads to $Zn^{2+}$ -dependent mitochondrial dysfunction

Cultures were loaded with the high affinity  $Zn^{2+}$  indicator FluoZin-3 ( $K_d \sim 15$  nM), Rhod123 or HET in  $0$   $Ca^{2+}$  HSS, then exposed to DTDP (60 or 100  $\mu$ M; to disrupt cytosolic  $Zn^{2+}$  buffering), with FCCP (1  $\mu$ M) or TPEN (20  $\mu$ M) applied as indicated. Traces represent mean  $\pm$  SEM  $F_x/F_0$  values for each indicator and represents 5 experiments consisting of 100 neurons. Grey bars indicate time points of comparison (\* indicates  $p < 0.05$ , \*\* indicates  $p < 0.01$ , \*\*\* indicates  $p < 0.001$ , by two-tailed t-test).

**A). DTDP induces dose-dependent cytosolic  $Zn^{2+}$  release and mitochondrial  $Zn^{2+}$  accumulation:** FluoZin-3 loaded neurons were exposed to DTDP followed by addition of FCCP, as indicated. Note the dose dependent effects of DTDP, with 100  $\mu$ M causing both greater cytosolic  $Zn^{2+}$  rise and mitochondrial  $Zn^{2+}$  loading (as indicated by the FCCP-induced  $F$ ) than 60  $\mu$ M.

**B). Disruption of buffering via DTDP can induce mitochondrial dysfunction:** Rhod123- (left) or HET- (right) loaded neurons were subjected to the indicated DTDP and FCCP exposures. Note that the 100  $\mu$ M DTDP exposure resulted in substantial loss of  $\Psi_{mito}$  within 25 min (as indicated by the minimal response to FCCP) and significant ROS production, while 60  $\mu$ M DTDP had far smaller effects.



**C). DTDP effects on mitochondria are Zn<sup>2+</sup>-dependent:** Rhod123- (**left**) or HET- (**right**) loaded neurons were exposed to 100  $\mu$ M DTDP  $\pm$  Zn<sup>2+</sup> chelator TPEN (applied 10 min before DTDP), followed by FCCP (only in Rhod123 loaded cultures), as indicated. Note that TPEN largely eliminated the DTDP induced loss of  $\Psi_{\text{mito}}$  (**left**) and markedly attenuated the ROS production (**right**).

Author Manuscript

Author Manuscript

Author Manuscript

Author Manuscript

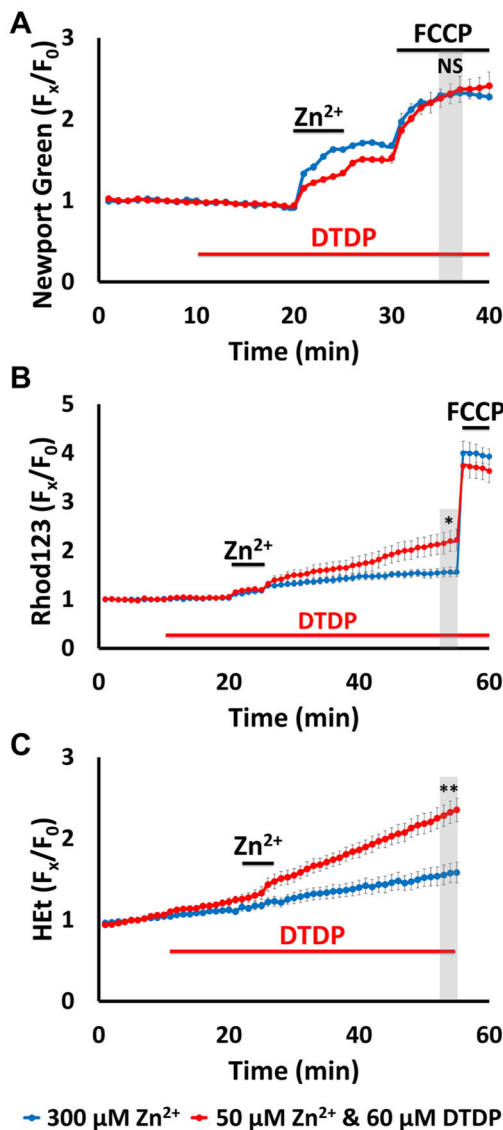


**Figure 3. Impaired cytosolic Zn<sup>2+</sup> buffering markedly enhances the acute impact of Zn<sup>2+</sup> exposures on mitochondria**

Cultures were loaded with Newport Green, Rhod123, or HET in 0 Ca<sup>2+</sup> HSS, and exposed to high K<sup>+</sup>/300 μM Zn<sup>2+</sup> alone (**blue**), or to high K<sup>+</sup>/50 μM Zn<sup>2+</sup> with 60 μM DTDP (applied as indicated; **red**); FCCP (1 μM) was added as indicated. Traces represent mean ± SEM F<sub>x</sub>/F<sub>0</sub> values for each dye and represents 6 experiments consisting of 120 neurons. Grey bars indicate time points of comparison (NS indicates No Significance, \* indicates p < 0.05, \*\* indicates p < 0.01, by two-tailed t-test).

**A). Low exogenous Zn<sup>2+</sup> exposure to neurons with impaired buffering results in similar degrees of mitochondrial uptake as much higher Zn<sup>2+</sup> exposure with intact buffering:** Note the similar magnitudes of mitochondrial Zn<sup>2+</sup> loading caused by the high K<sup>+</sup>/300 μM Zn<sup>2+</sup> (**blue**) and the high K<sup>+</sup>/50 μM Zn<sup>2+</sup>/DTDP exposures.

**B, C). However, the lower Zn<sup>2+</sup> exposure with impaired buffering results in greater mitochondrial dysfunction:** Rhod123 (**B**) or HET (**C**) loaded neurons were exposed as

indicated. Note that the 50  $\mu\text{M}$   $\text{Zn}^{2+}$ /DTDP exposure induced markedly greater loss of  $\psi_m$  and ROS generation than 300  $\mu\text{M}$   $\text{Zn}^{2+}$  alone.

Author Manuscript

Author Manuscript

Author Manuscript

Author Manuscript

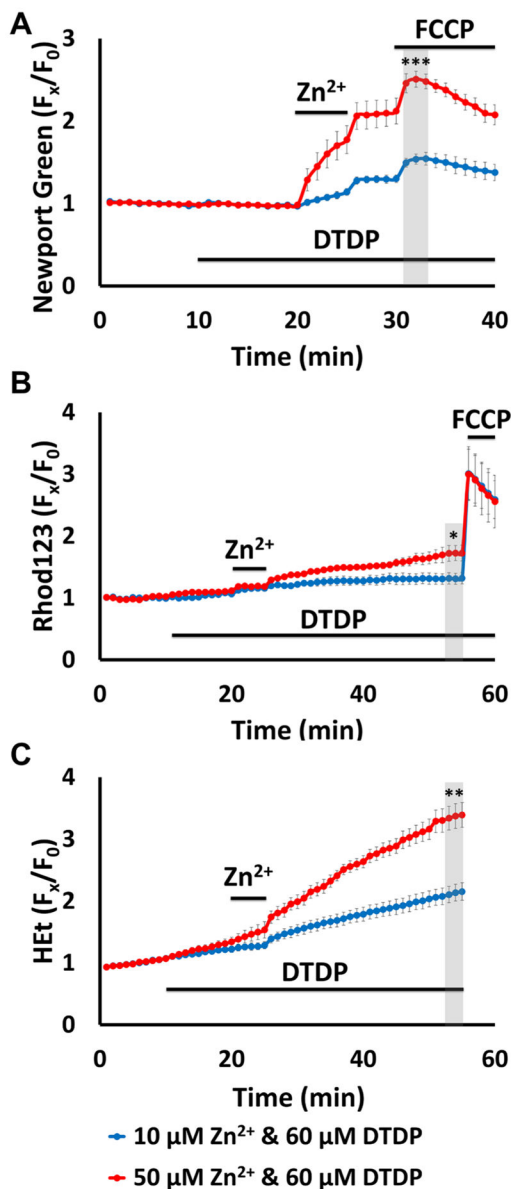


**Figure 4. Zn<sup>2+</sup> exposure dose-dependence of mitochondrial Zn<sup>2+</sup> loading and acute dysfunction in neurons with impaired buffering**

Cultures were loaded with Newport Green, Rhod123 or HET in 0 Ca<sup>2+</sup> HSS, and exposed to high K<sup>+</sup> with 10 (blue) or 50 (red) μM Zn<sup>2+</sup> in 60 μM DTDP. FCCP (1 μM) was added as indicated. Traces represent mean ± SEM F<sub>x</sub>/F<sub>0</sub> values for each dye and represents 6 experiments consisting of 120 neurons. Grey bars indicate time points of comparison (\* indicates p < 0.05, \*\* indicates p < 0.01, \*\*\* indicates p < 0.001, by two-tailed t-test).

**A). Zn<sup>2+</sup> exposure induces dose-dependent mitochondrial Zn<sup>2+</sup> loading in neurons with disrupted buffering:** Note the dose dependency of the cytosolic Zn<sup>2+</sup> rise and mitochondrial Zn<sup>2+</sup> uptake, with the 50 μM Zn<sup>2+</sup> exposure causing far greater Zn<sup>2+</sup> uptake than the 10 μM Zn<sup>2+</sup>.

**B, C). Mitochondrial dysfunction reflects the extent of Zn<sup>2+</sup> accumulation:** Rhod123 (**B**) or HEt (**C**) loaded neurons were exposed as indicated. Note that the 50  $\mu\text{M}$  Zn<sup>2+</sup> exposure induced far greater loss of  $\psi_m$  and ROS generation than 10  $\mu\text{M}$  Zn<sup>2+</sup>. Further note that despite causing relatively strong ROS generation, 50  $\mu\text{M}$  Zn<sup>2+</sup> still only caused modest loss of  $\psi_m$ .

Author Manuscript

Author Manuscript

Author Manuscript

Author Manuscript

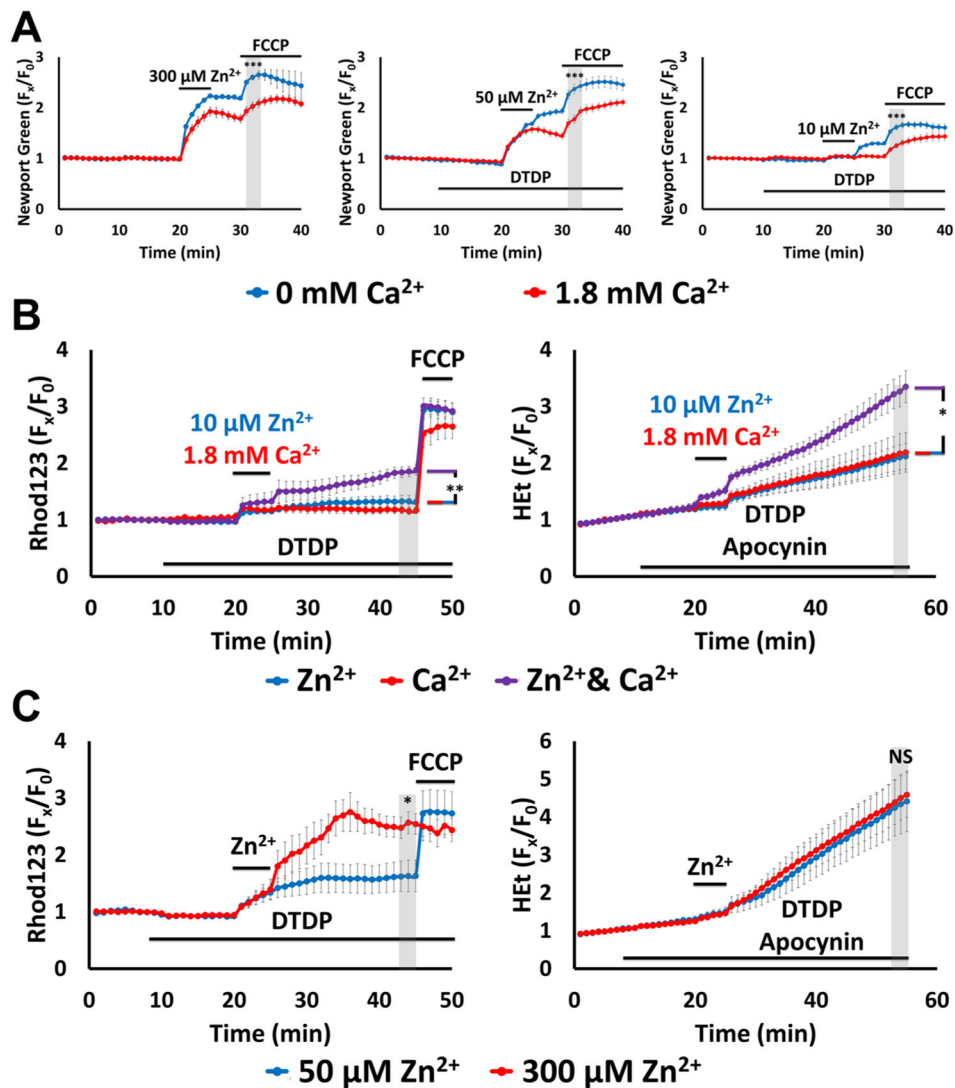


**Figure 5.  $\text{Ca}^{2+}$  attenuates mitochondrial  $\text{Zn}^{2+}$  accumulation despite exacerbating the consequent dysfunction**

Cultures were loaded with Newport Green, Rhod123 or HET in 0 or 1.8  $\text{Ca}^{2+}$  HSS, and exposed to high  $\text{K}^+$  with 300, 50, 10 or 0  $\mu\text{M Zn}^{2+}$  (as indicated, along with 10  $\mu\text{M MK-801}$ , to inhibit  $\text{Ca}^{2+}$ -entry via NMDA receptor activation); DTDP (60  $\mu\text{M}$ ), FCCP (1  $\mu\text{M}$ ) and/or apocynin (500  $\mu\text{M}$ ) were added as indicated. Traces represent mean  $\pm$  SEM  $F_x/F_0$  values for each dye and represents 5 experiments consisting of 120 neurons. Grey bars indicate time points of comparison (NS indicates No Significance, \* indicates  $p < 0.05$ , \*\* indicates  $p < 0.01$ , \*\*\* indicates  $p < 0.001$ , by two-tailed t-test [A, C] or by one-way ANOVA with Tukey post hoc [B]).

**A). Presence of  $\text{Ca}^{2+}$  decreases neuronal and mitochondrial  $\text{Zn}^{2+}$  uptake:** Note that presence of  $\text{Ca}^{2+}$  attenuated both cytosolic  $\text{Zn}^{2+}$  rise during the exposure and FCCP-induced mitochondrial  $\text{Zn}^{2+}$  release.

**B).  $\text{Ca}^{2+}$  and  $\text{Zn}^{2+}$  synergistically induce mitochondrial dysfunction:** Neurons loaded with Rhod123 (left) or HET (right) were exposed to high  $\text{K}^+$ /DTDP/MK-801 with 10  $\mu\text{M}$

Zn<sup>2+</sup> (**blue**), 1.8 mM Ca<sup>2+</sup> (**red**) or with both Zn<sup>2+</sup> and Ca<sup>2+</sup> (**purple**) for 5 min, then washed as indicated. Apocynin was added to HET-loaded neurons (**right**) to inhibit contributions from Ca<sup>2+</sup>-dependent NOX activation. Note that despite relatively little effects from Ca<sup>2+</sup> and Zn<sup>2+</sup> individually, together they induced significant mitochondrial dysfunction.

**C). Overwhelming mitochondrial Zn<sup>2+</sup> loading induces rapid mitochondrial depolarization:** Neurons loaded with Rhod123 (**left**) or HET (**right**) in 1.8 Ca<sup>2+</sup> HSS were exposed to high K<sup>+</sup>/DTDP/MK-801/Ca<sup>2+</sup>, with 50 (**blue**) or 300 μM (**red**) Zn<sup>2+</sup> for 5 min, followed by wash as indicated. Note that 300 μM Zn<sup>2+</sup> induced greater loss of  $\Psi_m$  than 50 μM Zn<sup>2+</sup>, despite both inducing similar levels of ROS generation.



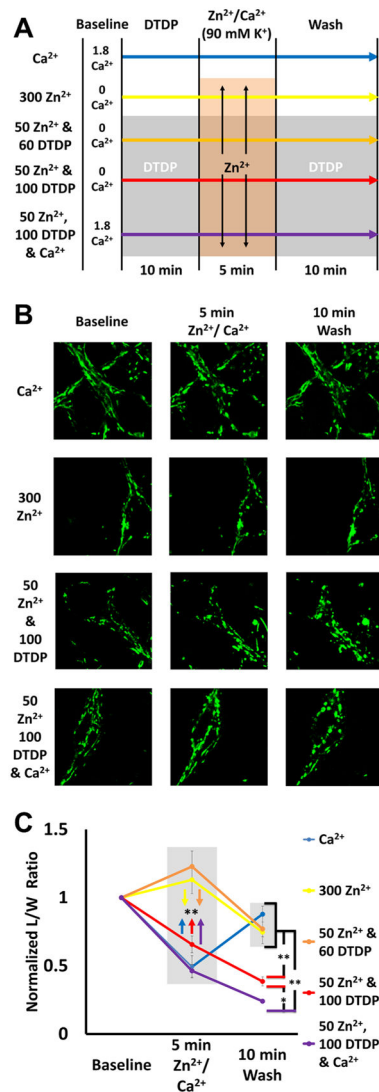


**Figure 6. Effects of Ca<sup>2+</sup>, Zn<sup>2+</sup>, and disruption of cytosolic Zn<sup>2+</sup> buffering on mitochondrial morphology**

**A). Experiment schematic:** Neurons loaded with the mitochondrial dye MitoTracker Green (200 nM) were placed in 0 or 1.8 Ca<sup>2+</sup> HSS, then exposed to DTDP (60 or 100 μM; where indicated), high K<sup>+</sup>/MK-801 with Zn<sup>2+</sup> (0, 50, or 300 μM) and/or 1.8 mM Ca<sup>2+</sup>, followed by wash into HSS ± DTDP, as described.

**B). Representative images:** Confocal images (1000x) were taken at baseline, 5 min after Zn<sup>2+</sup> and/or Ca<sup>2+</sup> exposure, and 10 min after wash.

**C). Zn<sup>2+</sup> and Ca<sup>2+</sup> induce different patterns of morphology change:** The length and width of individual mitochondria were measured blindly, and length/width (L/W) ratios calculated and normalized to baseline. Values for baseline, 5 min after exposure, and after 10 min wash are displayed. Traces show mean ± SEM normalized L/W ratio for each time point, each representing 5 experiments consisting of 50 mitochondria (\* indicates p < 0.05, \*\* indicates p < 0.01, by one-way ANOVA with Tukey post hoc). Note that while the

Ca<sup>2+</sup> induces a rapid but transient morphologic change, Zn<sup>2+</sup> triggers more progressive changes (that increase with the degree of Zn<sup>2+</sup> loading).

Author Manuscript

Author Manuscript

Author Manuscript

Author Manuscript

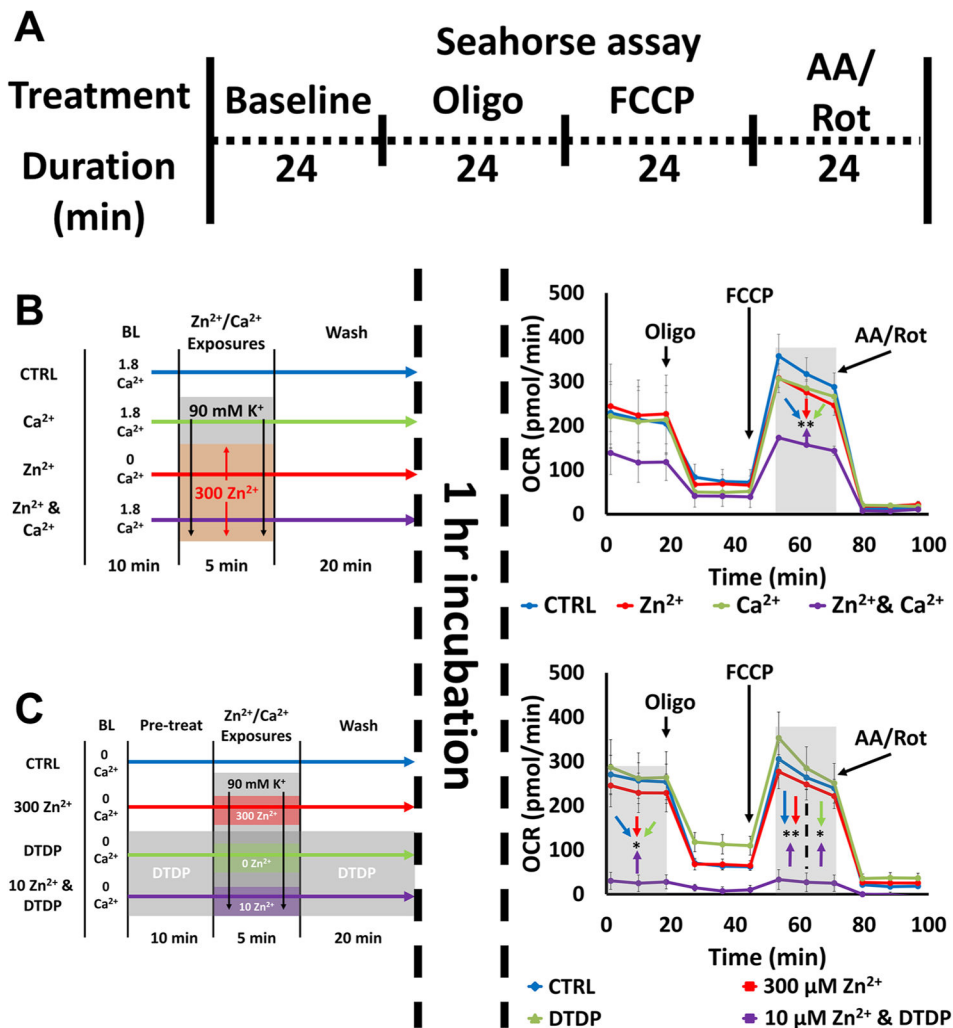


**Figure 7.  $Zn^{2+}$ -induced inhibition of mitochondrial respiration: synergy with  $Ca^{2+}$  and effects of disrupted buffering**

**A). Schematic of experiment:** Neurons were exposed to a series of treatments (detailed in **B** and **C**, left), incubated for 1 hr, then placed in the Seahorse assay, which measures  $O_2$  consumption rate (OCR) at baseline and after sequential application of oligomycin (**Oligo**; 1  $\mu M$ ), FCCP (2  $\mu M$ ), and antimycin A & rotenone (**AA/Rot**; both 1  $\mu M$ ) to characterize various respiratory parameters. Traces (**B** and **C**, right) show time course of OCR and represent mean  $\pm$  SEM of 3 separate experiments, each consisting of 3 – 4 wells of cultured neurons, with arrows indicating time point at which mitochondrial inhibitors were added. Grey bars indicate time points of comparison (\* indicates  $p < 0.05$ , \*\* indicates  $p < 0.01$ , by one-way ANOVA with Tukey post hoc).

**B).  $Ca^{2+}$  and  $Zn^{2+}$  synergistically inhibit mitochondrial respiration:** Neurons were placed in 0 or 1.8  $Ca^{2+}$  HSS, exposed to high  $K^+$ /MK-801 with 300  $\mu M$   $Zn^{2+}$ , 1.8 mM  $Ca^{2+}$  or both  $Zn^{2+}$  and  $Ca^{2+}$  as described (**left**). After 1 hr incubation OCR was measured (**right**). Note that simultaneous exposure to  $Zn^{2+}$  and  $Ca^{2+}$  induced significant inhibition of mitochondrial respiration, despite the ions having minimal effects individually.

**C). Disrupted Zn<sup>2+</sup> buffering significantly exacerbates Zn<sup>2+</sup> effects on mitochondrial respiration:** Neurons were placed in 0 Ca<sup>2+</sup> HSS, exposed to DTDP (100 μM; where indicated), high K<sup>+</sup>/MK-801 with Zn<sup>2+</sup> (300, 10 or 0 μM, as indicated; **left**). After 1 hr incubation OCR was measured (**right**). Note the near complete inhibition of mitochondrial respiration by 10 μM Zn<sup>2+</sup> exposure with DTDP.

Author Manuscript

Author Manuscript

Author Manuscript

Author Manuscript

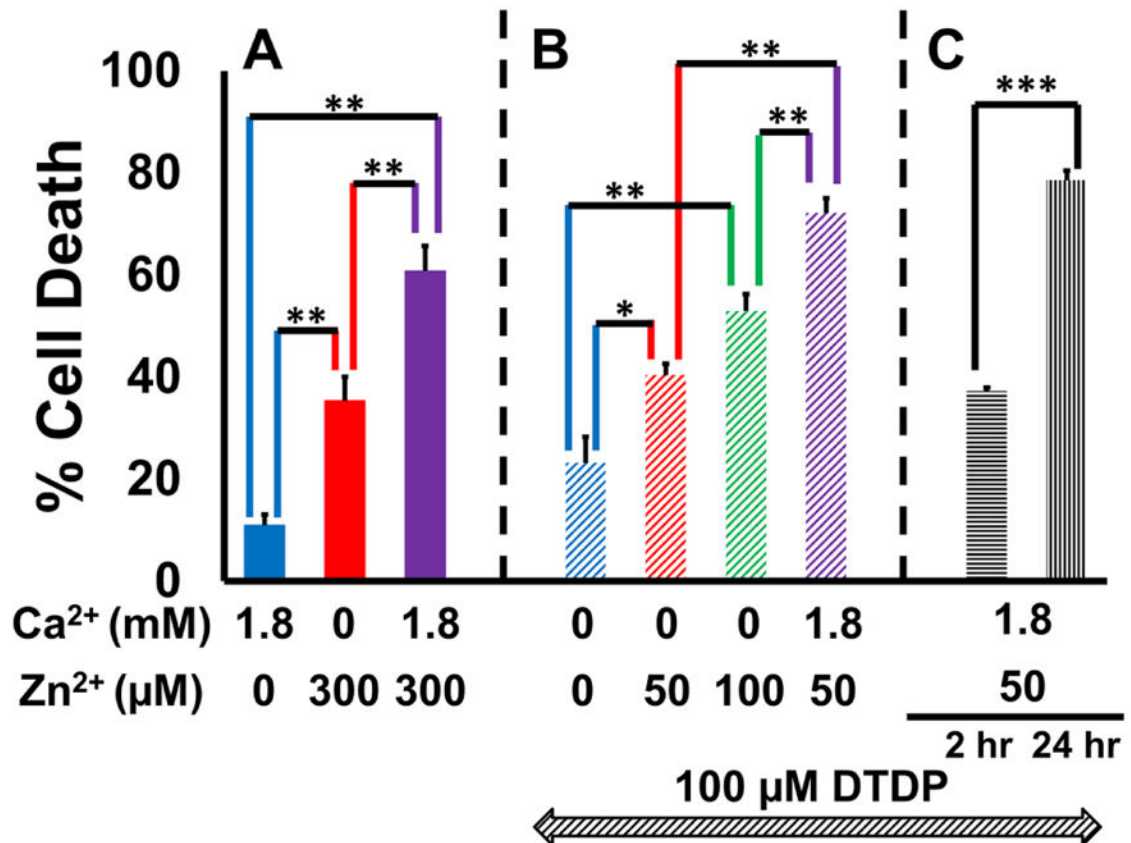


**Figure 8. Mitochondrial Zn<sup>2+</sup> accumulation contributes to neuron death**

Neurons were exposed to a sequence of 10 min DTDP (100 μM; as indicated in **B** and **C**), 5 min high K<sup>+</sup>/MK-801 exposures with Zn<sup>2+</sup> and/or Ca<sup>2+</sup> (concentration as shown), washed for 10 min (with DTDP in **B** and **C**), transferred to MEM + 25 mM glucose and returned to the incubator for 24 hrs (or for only 2 hrs where indicated in **C**), prior to assessing cell death via LDH efflux assay. Bars show % cell death (see Material and methods), and represent mean ± SEM of 3 independent experiments, each consisting of 4 wells of cultured neurons (\* indicates p < 0.05, \*\* indicates p < 0.01, \*\*\* indicates p < 0.001 by one-way ANOVA with Tukey post hoc [**A** and **B**] or by two-tailed t-test [**C**]).

**A). Ca<sup>2+</sup> and Zn<sup>2+</sup> synergistically induce cell death:** Note that while 300 μM Zn<sup>2+</sup> induced more cell death than 1.8 mM Ca<sup>2+</sup>, its impact was further exacerbated by the presence of Ca<sup>2+</sup>.

**B). Dose-dependency of Zn<sup>2+</sup>-induced cell death under conditions of strongly disrupted buffering:** Note the dose-dependent increase in cell death with increasing Zn<sup>2+</sup> exposures, that was further enhanced by the presence of Ca<sup>2+</sup>.

**C). Zn<sup>2+</sup>-induced cell death progresses gradually over hours:** Note the significantly greater cell death at 24 hrs compared to 2 hrs.

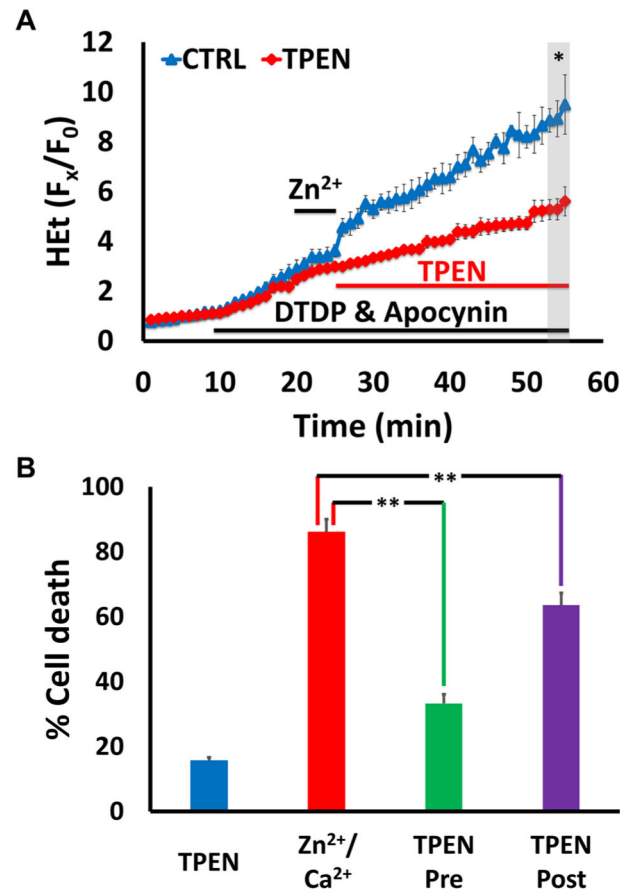


**Figure 9. Delayed Zn<sup>2+</sup> chelation attenuates mitochondrial ROS generation and neuron death** Neurons were exposed to high K<sup>+</sup>/50 μM Zn<sup>2+</sup>/MK-801, with DTDP (100 μM), and apocynin (500 μM, A only). TPEN was applied as indicated below. Traces (A) represent HET F<sub>x</sub>/F<sub>0</sub> and bars (B) represent % cell death after 24 hr; all values are mean ± SEM and represents 3 independent experiments. Grey bar (in A) indicates time points of comparison (\* indicates p < 0.05, \*\* indicates p < 0.01, by two-tailed t-test [A] or by one-way ANOVA with Tukey post hoc [B]).

**A). Delayed Zn<sup>2+</sup> chelation attenuates Zn<sup>2+</sup> triggered ROS production:** Note the rapid rise in HET F that was largely attenuated by TPEN (20 μM), added after the Zn<sup>2+</sup> exposure. **B). Zn<sup>2+</sup> chelation attenuates cell death even when delivered after the Zn<sup>2+</sup> exposure:** Cultured neurons were exposed as described, with TPEN (10 μM) present either for 10 min before, during and 10 min after high K<sup>+</sup>/Zn<sup>2+</sup> exposure (TPEN pre), or only for 10 min after Zn<sup>2+</sup> exposure (TPEN post). Cultures were then transferred to MEM + 25 mM glucose and returned to the incubator for 24 hrs, prior to assessing cell death via LDH efflux assay. Note that both the TPEN pre- and post-treatments attenuated neuron death.